# On the Energy–Delay Tradeoff and Relay Positioning of Wireless Butterfly Networks

Quoc-Tuan Vien, *Member, IEEE*, Huan X. Nguyen, *Member, IEEE*, Brian G. Stewart, *Member, IEEE*, Jinho Choi, *Senior Member, IEEE*, and Wanqing Tu, *Member, IEEE*

***Abstract*—This paper considers energy–delay tradeoff (EDT) of data transmission in wireless-network-coded butterfly networks (WNCBNs) where two sources convey their data to two destinations with the assistance of a relay employing either physical-layer network coding (PNC) or analog network coding (ANC). Hybrid automatic repeat request with incremental redundancy (HARQ-IR) is applied for reliable communication. In particular, we first investigate the EDT of both PNC and ANC schemes in WNCBNs to evaluate their energy efficiency. It is found that there is no advantage to using a relay in a high-power regime. However, in a low-power regime, the PNC scheme is shown to be more energy efficient than both the ANC and direct transmission (DT) schemes if the relay is located far from the sources, whereas both the PNC and ANC schemes are less energy efficient than the DT scheme when the relay is located near the sources. Additionally, algorithms that optimize relay positioning (RP) are developed based on two criteria: minimizing total transmission delays and minimizing total energy consumption subject to node location and power allocation constraints. This optimization can be considered a benchmark for RP in either a low-latency or low-energy-consumption WNCBN.**

***Index Terms*—Hybrid automatic repeat request with incremental redundancy (HARQ-IR), network coding (NC), wireless butterfly network.**

## I. Introduction

RECENTLY, the use of relaying techniques in wireless communications has attracted growing interest [1]–[3]. Relays can be used not only to increase coverage for remote transmissions but also to improve service quality and link capacity for local users [4], [5]. Inspired by the benefits of relays, relay-assisted communications are incorporated in various wireless system models such as cellular [4]–[6], *ad hoc* [7], and sensor [8] networks. Data transmission from source nodes to destination nodes is realized with the assistance of one or multiple relay nodes using either decode-and-forward or amplify-and-forward relaying protocols [3].

Basically, relays transmit packets through a store-and-forward mechanism and thus do not increase the network throughput. In an attempt to improve throughput, the concept of network coding (NC), which was initially proposed to increase the system throughput in lossless networks [9], [10], has been applied to relays to improve network throughput [11]–[15]. The principle of NC is that the relays perform algebraic linear/logic operations on received packets from multiple transmission source nodes and then forward the combined packets to the destination nodes in the subsequent transmissions. An appropriate NC employment at the relay nodes could save bandwidth for a higher system throughput. Many NC-based protocols have been proposed and investigated for particular relay topologies such as relay-assisted bidirectional channels [16], broadcast channels [17], multicast channels [18], unicast channels [19], and vehicular networks [20], [21]. As a specific model of multicast channels, butterfly networks have been investigated, e.g., in [22]–[25], in which NC is applied at the relay node to help two source nodes simultaneously transmit their information to two destination nodes.

In addition to the merit of NC techniques providing throughput improvement, the reliability and energy efficiency of data transmission should be also taken into consideration within communication systems. This is particularly the case in wireless environments where the communication channels often suffer from deep fading and background noise, and where the energy consumption of various communication and networking devices causes an increasing carbon dioxide emission. To cope with the reliability issue, hybrid automatic repeat request (HARQ) protocols were proposed to reliably deliver information over error-prone channels such as the wireless medium [26]. Specifically, HARQ with incremental redundancy (HARQ-IR) has been shown to achieve the ergodic capacity of fading and interference channels [27], [28]. With respect to energy efficiency, energy–delay tradeoff (EDT) tools have been developed in [29] to evaluate the energy efficiency of HARQ-IR protocols for NC-based two-way relay systems. However, for NC-based multisource-multidestination relay networks [30], [31], the EDT of HARQ-IR protocols has received little attention in the literature.

Manuscript received June 27, 2013; revised April 14, 2014; accepted April 14, 2014. Date of publication April 30, 2014; date of current version January 13, 2015. This work was supported in part by the U.K. Engineering and Physical Sciences Research Council under Grant EP/J017159/1, by the British Council Research Link Programme under Project 101468, and by the Gwanju Institute of Science and Technology International College under the 2013 GUP Research Fund. The review of this paper was coordinated by Dr. M. Elkashlan.

Q.-T. Vien and H. X. Nguyen are with the School of Science and Technology, Middlesex University, NW4 4BT London, U.K. (e-mail: q.vien@mdx.ac.uk; h.nguyen@mdx.ac.uk).

B. G. Stewart is with the School of Engineering and Built Environment, Glasgow Caledonian University, G4 0BA Glasgow, U.K. (e-mail: b.stewart@gcu.ac.uk).

J. Choi is with the School of Information and Communications, Gwangju Institute of Science and Technology, Gwangju 500-712, Korea (e-mail: jchoi0114@gist.ac.kr).

W. Tu is with the School of Computing Science and Digital Media, The Robert Gordon University, AB10 7GJ Aberdeen, U.K. (e-mail: w.tu@rgu.ac.uk).

Color versions of one or more of the figures in this paper are available online at http://ieeexplore.ieee.org.

Digital Object Identifier 10.1109/TVT.2014.2321229

In this paper, we investigate the energy efficiency for a reliable wireless-network-coded butterfly network (WNCBN), which consists of two source nodes, one relay node, and two destination nodes. The reliability of all communication links is guaranteed by the HARQ-IR protocol. The relay node in a WNCBN carries out either physical-layer NC (PNC) [12] or analog NC (ANC) [13] on the signals received from two source nodes before forwarding to the destination nodes. This paper is an extension of [32] in which we briefly investigated the energy efficiency for a reliable WNCBN. In this paper, for completeness, we first provide the expression of the EDTs for the HARQ-IR protocols with PNC and ANC schemes in WNCBNs. To provide insight into the derived expressions, approximations of the EDTs for various HARQ-IR protocols are derived in high- and low-power regimes. In the high-power regime, the relay in the relay-aided transmission is shown to have no advantage over the direct transmission (DT) scheme.[1] In the low-power regime, we show that, with equal power allocation and when the relay node is located far from the source nodes, the PNC scheme is more energy efficient than both the ANC and DT schemes. However, when the relay node is located near the source nodes, it is demonstrated that the DT scheme performs better in terms of energy efficiency than both PNC and ANC schemes.

Another contribution of this paper is that we develop new algorithms to optimize relay positioning (RP) based on the derived EDT for each NC scheme in a WNCBN. The objectives of optimized RP are to find the position for the relay node that can minimize either the total delay or the total energy consumption in the whole system, given the constraints on power allocation and the locations of source and destination nodes. We then achieve the following findings from this positioning design.

- *Minimum total delay*: In the case of equal power allocation at the source nodes, the ANC-based relay should be located nearer to the destination nodes than the PNC-based relay if the power at the source nodes is larger than the power at the relay; otherwise, the ANC-based relay should be located closer to the source nodes than the PNC-based relay. For the scenario of unequal power allocation at the source nodes, the ANC-based relay should be positioned near the lower power source node, whereas the PNC-based relay should be located in the region between the lower power source node and the nearby destination node.
- *Minimum total energy consumption*: In the case of equal power allocation at the source nodes, the ANC-based relay should be close to the destination nodes, whereas the PNC-based relay should stay close to the source nodes if the power at the source nodes is larger than the power at the relay; otherwise, the ANC-based and PNC-based relays should be close to the source and the destination nodes, respectively. For the scenario of unequal power allocation at the source nodes, the ANC-based and the PNC-based relays should be located in the same region as for the minimum total delay.

[1]The DT scheme refers to the model in which two sources simultaneously transmit information to the destinations without using relaying techniques.

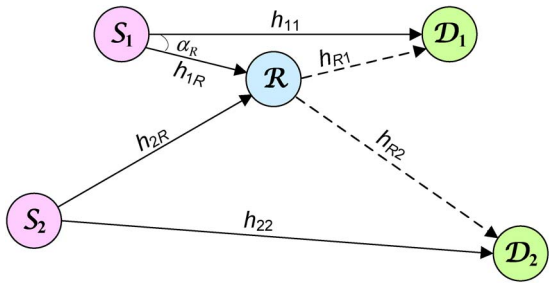


Fig. 1. System model of wireless butterfly network.

Interestingly, we observe that the ANC-based relay can be located within a small region to nearly achieve both the minimum total delay and the minimum total energy consumption, whereas the optimized locations for the PNC-based relay vary depending on the objective functions.

The remainder of this paper is organized as follows. In Section II, we introduce the system model of WNCBNs and the EDT of the HARQ-IR protocol for a simple single-source–single-destination communication system. Section III derives the EDTs of the HARQ-IR protocols in WNCBNs using PNC and ANC schemes. Section IV provides the approximated expressions of the EDTs for various HARQ-IR protocols in high- and low-power regimes. The optimization method for relay locations is presented in Section V. Numerical results are presented and discussed in Section VI. Finally, Section VII concludes this paper.

## II. System Model, Hybrid Automatic Repeat Request With Incremental Redundancy Protocol, and Energy–Delay Tradeoff

Here, we introduce the system model of WNCBN and the HARQ-IR protocol for reliable communications and the associated energy–delay relation.

### A. System Model of WNCBN

The basic system model of a WNCBN is shown in Fig. 1 where data transmitted from two source nodes $\mathcal{S}_1$ and $\mathcal{S}_2$ to two destination nodes $\mathcal{D}_1$ and $\mathcal{D}_2$ are assisted by one relay node $\mathcal{R}$. A half-duplex WNCBN system is considered where all nodes can either transmit or receive data, but not simultaneously. In the WNCBN, the NC is applied at $\mathcal{R}$ to help $\mathcal{S}_1$ and $\mathcal{S}_2$ simultaneously transmit their data packets $\mathbf{s}_1$ and $\mathbf{s}_2$, respectively, to $\mathcal{D}_1$ and $\mathcal{D}_2$ in two time slots. In the first time slot, $\mathcal{S}_1$ transmits $\mathbf{s}_1$ to both $\mathcal{R}$ and $\mathcal{D}_1$, whereas $\mathcal{S}_2$ transmits $\mathbf{s}_2$ to both $\mathcal{R}$ and $\mathcal{D}_2$. Then, $\mathcal{R}$ performs NC on the mixed signals received from $\mathcal{S}_1$ and $\mathcal{S}_2$ and broadcasts the network-coded signals to both $\mathcal{D}_1$ and $\mathcal{D}_2$ in the second time slot. Accordingly, $\mathcal{D}_1$ can extract the signal transmitted from $\mathcal{S}_2$ (i.e., $\mathbf{s}_2$), and $\mathcal{D}_2$ can extract the signal transmitted from $\mathcal{S}_1$ (i.e., $\mathbf{s}_1$). The data transmission in the first time slot consists of two DTs ($\mathcal{S}_1 \rightarrow \mathcal{D}_1$ and $\mathcal{S}_2 \rightarrow \mathcal{D}_2$) and a multiple access (MA) transmission ($\{\mathcal{S}_1\ \mathcal{S}_2\} \rightarrow \mathcal{R}$),[2] whereas there is only a broadcast (BC)

[2]It is noted that DT and MA transmissions are carried out simultaneously in the first time slot with the same coding scheme due to the broadcast nature of the wireless medium.

TABLE I
SUMMARY OF MAIN NOTATION

| Notation | Meaning |
|---|---|
| $d_{AB}$, $\{A,B\} \in \{S_1, S_2, R, D_1, D_2\}$ | distance of link $\mathcal{A}-\mathcal{B}$ |
| $\alpha_1$, $\alpha_2$, $\alpha_3$, $\alpha_4$, $\alpha_R$ | physical angles $\widehat{\mathcal{D}_1\mathcal{S}_1\mathcal{S}_2}$, $\widehat{\mathcal{S}_1\mathcal{S}_2\mathcal{D}_2}$, $\widehat{\mathcal{S}_2\mathcal{D}_2\mathcal{D}_1}$, $\widehat{\mathcal{D}_2\mathcal{D}_1\mathcal{S}_1}$, $\widehat{\mathcal{D}_1\mathcal{S}_1\mathcal{R}}$, respectively |
| $P_i$, $i=1,2$, $P_R$ | transmit powers of $\mathcal{S}_i$,$\mathcal{R}$, respectively |
| $r_i$, $i=1,2$, $r_R$ | transmission rate at $\mathcal{S}_i$, $\mathcal{R}$, respectively |
| $h_{ii}$, $h_{iR}$, $h_{Ri}$, $i=1,2$ | channel coefficients of links $\mathcal{S}_i \to \mathcal{D}_i$, $\mathcal{S}_i \to \mathcal{R}$, $\mathcal{R} \to \mathcal{D}_i$, respectively |
| $\mathbf{n}_{ii}$, $\mathbf{n}_R$, $\mathbf{n}_{Ri}$, $i=1,2$ | independent circularly symmetric complex Gaussian (CSCG) noise vectors of links $\mathcal{S}_i \to \mathcal{D}_i$, $\{\mathcal{S}_1,\mathcal{S}_2\} \to \mathcal{R}$, $\mathcal{R} \to \mathcal{D}_i$, respectively, with each entry having zero mean and unit variance |
| $\gamma_{ii}$, $\gamma_{iR}$, $\gamma_{Ri}$, $i=1,2$ | signal-to-noise ratio (SNR) of links $\mathcal{S}_i \to \mathcal{D}_i$, $\mathcal{S}_i \to \mathcal{R}$, $\mathcal{R} \to \mathcal{D}_i$, respectively |
| $\nu$ | pathloss exponent between a pair of transceiver nodes |
| $\kappa_{(\cdot)}$ | number of transmissions required in HARQ-IR protocol to transmit a data packet |
| $\delta_{(\cdot)}$ | effective delay (ED) of HARQ-IR protocol |
| $\epsilon_{(\cdot)}$ | energy per bit (EB) of HARQ-IR protocol |
| $[a]_i$ | $i$-th realisation of a random variable $a$ |
| $\bar{a}$ | mean of a random variable $a$ |
| $\log(\cdot)$ | binary logarithm function |
| $\ln(\cdot)$ | natural logarithm function |
| $E[\cdot]$ | statistical expectation function |

transmission ($\mathcal{R} \to \{\mathcal{D}_1\ \mathcal{D}_2\}$) in the second time slot. In this paper, we focus on energy efficiency for a conventional butterfly network when the relay plays a role of coverage extension, to facilitate message delivery of indirect links ($\mathcal{S}_1 \to \mathcal{D}_2$ and $\mathcal{S}_2 \to \mathcal{D}_1$) but not to achieve diversity gain (although it can be achieved with appropriate technique). Therefore, we assume there is no direct link between $\mathcal{S}_1$ and $\mathcal{D}_2$ and between $\mathcal{S}_2$ and $\mathcal{D}_1$.

For convenience, the main notation used in this paper is listed in Table I.

### *B. HARQ-IR Protocol and EDT for Reliable Point-to-Point Communications*

To investigate the HARQ-IR protocols with PNC and ANC in WNCBNs, let us first introduce briefly a simple HARQ-IR protocol for point-to-point (P2P) communications [27] along with the EDT evaluation for this system model [29].

Over a P2P communication channel $\mathcal{S} \to \mathcal{D}$ employing the HARQ-IR protocol, node $\mathcal{S}$ encodes a data packet $\mathbf{d}$ into a sequence of $N$ coded packets $\{\mathbf{c}_1, \mathbf{c}_2, \ldots, \mathbf{c}_N\}$. Then, $\mathcal{S}$ sequentially transmits $\mathbf{c}_k$, $k=1,2,\ldots,N$, to $\mathcal{D}$ until a positive acknowledgement (ACK) is received. The signal $\mathbf{y}_k$ received at node $\mathcal{D}$ when transmitting the $k$th coded packet $\mathbf{c}_k$ from node $\mathcal{S}$ can be expressed through

$$\mathbf{y}_k = \sqrt{P} h_k \mathbf{x}_k + \mathbf{n}_k \tag{1}$$

where $P$ is the signal power, $h_k$ is the channel gain of link $\mathcal{S} \to \mathcal{D}$ for the $k$th packet transmission, $\mathbf{x}_k$ is the modulated signal of $\mathbf{c}_k$, and $\mathbf{n}_k$ is an independent circularly symmetric complex Gaussian (CSCG) noise vector with each entry having zero mean and unit variance.

Let $\kappa_{\mathrm{P2P}}$ denote the number of transmissions required in the HARQ-IR protocol to transmit a data packet from $\mathcal{S}$ to $\mathcal{D}$. $\kappa_{\mathrm{P2P}}$ can be expressed by [27]

$$\kappa_{\mathrm{P2P}} = \min\left\{ k \Big| \sum_{j=1}^{k} \log\left(1 + P\,|[h_k]_j|^2\right) > r_{\mathrm{P2P}} \right\} \tag{2}$$

where $r_{\mathrm{P2P}}$ denotes the initial rate of a capacity-achieving code in P2P communications. By using the same evaluation tool in [29], the EDT can be characterized by two normalized metrics: energy per bit (EB) (in J/b/Hz) and effective delay (ED) (in s/b/Hz). Here, the EB and ED are normalized over the transmission data rate $r_{\mathrm{P2P}}$. Let $\delta_{\mathrm{P2P}}$ and $\epsilon_{\mathrm{P2P}}$ denote ED and EB, respectively, of the HARQ-IR protocol for P2P communications. These metrics are given as

$$\delta_{\mathrm{P2P}} = \frac{\bar{\kappa}_{\mathrm{P2P}}}{r_{\mathrm{P2P}}} \tag{3}$$

$$\epsilon_{\mathrm{P2P}} = \frac{P\bar{\kappa}_{\mathrm{P2P}}}{r_{\mathrm{P2P}}} = P\delta_{\mathrm{P2P}} \tag{4}$$

where $\bar{\kappa}_{\mathrm{P2P}}$ denotes the average number of transmissions for reliable P2P communications.

## III. ENERGY–DELAY TRADEOFF IN WIRELESS-NETWORK-CODED BUTTERFLY NETWORKS

Basically, the signal processing at relay $\mathcal{R}$ can be carried out with either PNC or ANC protocols. Here, the EDTs of the HARQ-IR protocols with PNC and ANC are derived for the WNCBNs, as shown in Fig. 1.

### *A. EDT of HARQ-IR Protocol With PNC*

Using the PNC scheme for HARQ-IR in WNCBNs, $\mathcal{R}$ performs joint decoding of two signals received from $\mathcal{S}_1$ and $\mathcal{S}_2$ in the MA transmission [33]. Thus, the number of transmissions in the MA transmission can be determined through the MA channel capacity bound [34] as follows:

$$\begin{aligned}\kappa_{\mathrm{PNC,MA}} &= \min\left\{ k \Big| \left\{ \sum_{j=1}^{k} \log\left(1+[\gamma_{1R}]_j\right) < r_1 \right\} \right. \\ &\quad \cap \left\{ \sum_{j=1}^{k} \log\left(1+[\gamma_{2R}]_j\right) < r_2 \right\} \\ &\quad \left. \cap \left\{ \sum_{j=1}^{k} \log\left(1+[\gamma_{1R}]_j+[\gamma_{2R}]_j\right) < r_1+r_2 \right\} \right\}\end{aligned} \tag{5}$$

where $\gamma_{iR}$ and $r_i$, $i = 1, 2$, denote the SNR of the transmission link $\mathcal{S}_i \to \mathcal{R}$ and the transmission rate at $\mathcal{S}_i$, respectively. In parallel with the MA transmission, $\mathcal{D}_i$, $i = 1, 2$, receives the packet from $\mathcal{S}_i$ in the DR transmission. The received signal at $\mathcal{D}_i$ can be written as

$$\mathbf{y}_{ii} = \sqrt{P_i} h_{ii} \mathbf{s}_i + \mathbf{n}_{ii} \tag{6}$$

where $P_i$, $h_{ii}$, and $\mathbf{n}_{ii}$ denote the transmission power, channel coefficient, and CSCG noise vector at $\mathcal{D}_i$ of the transmission link $\mathcal{S}_i \to \mathcal{D}_i$, respectively. Similar to the transmission over P2P channels, the number of transmissions required at $\mathcal{S}_i$, $i = 1, 2$, to transmit $\mathbf{s}_i$ to $\mathcal{D}_i$ in the DR transmission can be computed as follows:

$$\kappa_{\mathrm{PNC,DR}_i} = \min \left\{ k \middle| \sum_{j=1}^{k} \log\left(1 + [\gamma_{ii}]_j\right) > r_i \right\} \tag{7}$$

where $\gamma_{ii}$ denotes the SNR of the transmission link $\mathcal{S}_i \to \mathcal{D}_i$. With the HARQ-IR protocol, the data packet is retransmitted by $\mathcal{S}_i$, $i = 1, 2$, until both $\mathcal{R}$ and $\mathcal{D}_i$ successfully decode. Thus, the number of transmissions at $\mathcal{S}_i$ and the total number of transmissions in the first time slot are given as follows:

$$\kappa_{\mathrm{PNC},S_i} = \max\left\{\kappa_{\mathrm{PNC,MA}}, \kappa_{\mathrm{PNC,DR}_i}\right\} \tag{8}$$

$$\kappa_{\mathrm{PNC},1} = \max\left\{\kappa_{\mathrm{PNC,MA}}, \kappa_{\mathrm{PNC,DR}_1}, \kappa_{\mathrm{PNC,DR}_2}\right\} \tag{9}$$

respectively. Then, $\mathcal{R}$ encodes the superimposed packet and then broadcasts the encoded packet to both $\mathcal{S}_1$ and $\mathcal{S}_2$ in the second time slot. The number of transmissions required at $\mathcal{R}$ to transmit the mixed packet to $\mathcal{D}_i$, $i = 1, 2$, in the BC transmission is similarly determined as in P2P communications, i.e.,

$$\kappa_{\mathrm{PNC,BC}_i} = \min \left\{ k \middle| \sum_{j=1}^{k} \log\left(1 + [\gamma_{Ri}]_j\right) > r_{i'} \right\} \tag{10}$$

where $i' = 1$ if $i = 2$ and $i' = 2$ if $i = 1$ (or $i' = i - (-1)^i$). Here, $\gamma_{Ri}$ denotes the SNR of the transmission link $\mathcal{R} \to \mathcal{D}_i$. To help both $\mathcal{D}_1$ and $\mathcal{D}_2$ detect the data packets from $\mathcal{S}_2$ and $\mathcal{S}_1$, respectively, $\mathcal{R}$ retransmits the packet until both $\mathcal{D}_1$ and $\mathcal{D}_2$ successfully detect it. Thus, the number of transmissions in the second time slot is computed by

$$\kappa_{\mathrm{PNC},2} = \max\left\{\kappa_{\mathrm{PNC,BC}_1}, \kappa_{\mathrm{PNC,BC}_2}\right\}. \tag{11}$$

Overall, the resulting ED and EB of the HARQ-IR protocol with the PNC are, respectively, given as follows:

$$\delta_{\mathrm{PNC}} = \frac{\bar{\kappa}_{\mathrm{PNC},1} + \bar{\kappa}_{\mathrm{PNC},2}}{r_1 + r_2} \tag{12}$$

$$\epsilon_{\mathrm{PNC}} = \frac{P_1 \bar{\kappa}_{\mathrm{PNC},S_1} + P_2 \bar{\kappa}_{\mathrm{PNC},S_2} + P_R \bar{\kappa}_{\mathrm{PNC},2}}{r_1 + r_2} \tag{13}$$

where $P_R$ denotes the transmission power at $\mathcal{R}$.

### B. EDT of HARQ-IR Protocol With ANC

With the ANC protocol, in the MA transmission of the first time slot, $\mathcal{R}$ receives the data packets from both $\mathcal{S}_1$ and $\mathcal{S}_2$, which can be written as follows:

$$\mathbf{r} = \sqrt{P_1} h_{1R} \mathbf{s}_1 + \sqrt{P_2} h_{2R} \mathbf{s}_2 + \mathbf{n}_R \tag{14}$$

where $h_{iR}$ and $\mathbf{n}_R$ denote the channel coefficient and the CSCG noise vector at $\mathcal{R}$ of the transmission link $\mathcal{S}_i \to \mathcal{R}$, respectively. At the same time, $\mathcal{D}_i$, $i = 1, 2$, receives the data packet from $\mathcal{S}_i$ in the DR transmission. Similarly, the received signal $\mathbf{y}_{ii}$ at $\mathcal{D}_i$ is given by (6), and the number of transmissions $\kappa_{\mathrm{ANC,DR}_i}$ is determined as $\kappa_{\mathrm{PNC,DR}_i}$ in (7).

Prior to broadcasting the received signal to both $\mathcal{D}_1$ and $\mathcal{D}_2$, $\mathcal{R}$ normalizes its received signal $\mathbf{r}$ in (14) by a factor $\lambda = 1/\sqrt{E[|\mathbf{r}|^2]} = 1/\sqrt{\gamma_{1R} + \gamma_{2R} + 1}$ to have unit average energy. Thus, in the BC transmission, the signals received at $\mathcal{D}_i$, $i = 1, 2$, can be written as

$$\mathbf{y}_{Ri} = \sqrt{P_R} h_{Ri} \lambda \mathbf{r} + \mathbf{n}_{Ri} \tag{15}$$

where $h_{Ri}$ and $\mathbf{n}_{Ri}$ denote the channel coefficient and CSCG noise vector at $\mathcal{D}_i$ of the transmission link $\mathcal{R} \to \mathcal{D}_i$, respectively. Then, $\mathcal{D}_i$, $i = 1, 2$, detects $\mathbf{s}_{i'}$, $i' = i - (-1)^i$, by canceling $\mathbf{s}_i$ which is detected in the DR transmission. The resulting SNR $\gamma_{i'}$ at $\mathcal{D}_i$ is expressed as follows:

$$\gamma_{i'} = \frac{\gamma_{Ri}\gamma_{i'R}}{\gamma_{Ri} + \gamma_{i'R} + \gamma_{iR} + 1} \tag{16}$$

where $\gamma_{iR}$ and $\gamma_{Ri}$ denote the SNRs of the transmission links $\mathcal{S}_i \to \mathcal{R}$ and $\mathcal{R} \to \mathcal{D}_i$, respectively. In the HARQ-IR protocol with ANC, $\mathcal{D}_1$ and $\mathcal{D}_2$ feedback to $\mathcal{S}_1$ and $\mathcal{S}_2$ over direct links to acknowledge the packets $\mathbf{s}_1$ and $\mathbf{s}_2$, respectively. Since there is no decoding process carried out at $\mathcal{R}$ in the first time slot, $\mathcal{R}$ does not perform any feedback for the links $\mathcal{S}_1 \to \mathcal{R}$ and $\mathcal{S}_2 \to \mathcal{R}$. However, $\mathcal{R}$ can help $\mathcal{D}_1$ and $\mathcal{D}_2$ forward the ACK of the packets $\mathbf{s}_2$ and $\mathbf{s}_1$ to $\mathcal{S}_2$ and $\mathcal{S}_1$, respectively. Therefore, the number of transmissions required at $\mathcal{S}_i$, $i = 1, 2$, to transmit $\mathbf{s}_i$ to $\mathcal{D}_{i'}$ is determined by the following:

$$\kappa_{\mathrm{ANC}_i} = \min \left\{ k \middle| \sum_{j=1}^{k} \log\left(1 + [\gamma_i]_j\right) > r_i \right\}. \tag{17}$$

The total number of transmissions at $\mathcal{S}_i$, $i = 1, 2$, is accordingly given as follows:

$$\kappa_{\mathrm{ANC},S_i} = \max\left\{\kappa_{\mathrm{ANC}_i}, \kappa_{\mathrm{ANC,DR}_i}\right\}. \tag{18}$$

It is noted that, with the ANC protocol, the retransmission of the lost packets at $\mathcal{D}_1$ and $\mathcal{D}_2$ is carried out by $\mathcal{S}_1$ and $\mathcal{S}_2$. $\mathcal{R}$ only amplifies and forwards to $\mathcal{D}_1$ and $\mathcal{D}_2$ the data received from $\mathcal{S}_1$ and $\mathcal{S}_2$. This means that the number of transmissions at $\mathcal{R}$ to assist $\mathcal{S}_1$ and $\mathcal{S}_2$ is also given as $\kappa_{\mathrm{ANC}_1}$ and $\kappa_{\mathrm{ANC}_2}$, respectively, and $\mathcal{R}$ uses half power for each task. Therefore, the resulting ED and EB of the HARQ-IR protocol with the ANC scheme are, respectively, obtained as

$$\delta_{\mathrm{ANC}} = \frac{\max\left\{\bar{\kappa}_{\mathrm{ANC},S_1}, \bar{\kappa}_{\mathrm{ANC},S_2}\right\} + \max\left\{\bar{\kappa}_{\mathrm{ANC}_1}, \bar{\kappa}_{\mathrm{ANC}_2}\right\}}{r_1 + r_2} \tag{19}$$

$$\epsilon_{\mathrm{ANC}} = \frac{P_1 \bar{\kappa}_{\mathrm{ANC},S_1} + P_2 \bar{\kappa}_{\mathrm{ANC},S_2} + \frac{P_R}{2} \bar{\kappa}_{\mathrm{ANC}_1} + \frac{P_R}{2} \bar{\kappa}_{\mathrm{ANC}_2}}{r_1 + r_2}. \tag{20}$$

## IV. Analysis of Energy-Delay Tradeoff in Wireless-Network-Coded Butterfly Networks

Here, we derive the approximations of the EDTs for various HARQ-IR protocols in WNCBNs in high- and low-power regimes. For comparison, both relay-aided transmission (i.e., PNC and ANC) and nonrelay-aided transmission (i.e., DT) are considered. Our comparison with the DT scheme is relative but can be justified because of the following: Both relay-aided transmission (i.e., PNC and ANC schemes) and nonrelay-aided transmission (i.e., DT scheme) require the same number of time slots to transmit data packets $\mathbf{s}_1$ and $\mathbf{s}_2$ from $\mathcal{S}_1$ and $\mathcal{S}_2$, respectively, to both $\mathcal{D}_1$ and $\mathcal{D}_2$. Specifically, in the DT scheme, in the $i$th, $i = 1, 2$, time slot $\mathcal{S}_i$ transmits $\mathbf{s}_i$ to $\mathcal{D}_1$ and $\mathcal{D}_2$ over $\mathcal{S}_i$-$\mathcal{D}_1$ and $\mathcal{S}_i$-$\mathcal{D}_2$ links, respectively. In the PNC and ANC schemes, the data transmission in the first time slot consists of two DTs ($\mathcal{S}_1 \to \mathcal{D}_1$ and $\mathcal{S}_2 \to \mathcal{D}_2$) and an MA transmission ($\{\mathcal{S}_1\ \mathcal{S}_2\} \to \mathcal{R}$), whereas there is only a BC transmission ($\mathcal{R} \to \{\mathcal{D}_1\ \mathcal{D}_2\}$) in the second time slot. This means that all the PNC, ANC, and DT schemes require two time slots for the data transmission, which proves a relatively fair comparison between these schemes.

Let $P$ denote the total power constraint of all transmitting nodes, i.e., $P = P_1 + P_2 + P_R$. Moreover, let us denote $\rho_1$, $\rho_2$, and $(1 - \rho_1 - \rho_2)$ as the fractions of power allocated to $\mathcal{S}_1$, $\mathcal{S}_2$, and $\mathcal{R}$, respectively.[3] Accordingly, $P_1 = \rho_1 P$, $P_2 = \rho_2 P$, and $P_R = (1 - \rho_1 - \rho_2)P$. All channel links are assumed to suffer from quasi-static Rayleigh block fading with $E[|h_{11}|^2] = 1/d^{\nu}_{S_1D_1}$, $E[|h_{22}|^2] = 1/d^{\nu}_{S_2D_2}$, $E[|h_{iR}|^2] = 1/d^{\nu}_{S_iR}$, and $E[|h_{Rj}|^2] = 1/d^{\nu}_{RD_j}$, $i = 1, 2$, $j = 1, 2$.

Using the HARQ-IR protocol with the DT scheme in WNCBN, the ED and EB can be simply derived as

$$\delta_{\mathrm{DT}} = \frac{\bar{\kappa}_{\mathrm{DT},1} + \bar{\kappa}_{\mathrm{DT},2}}{r_1 + r_2} \tag{21}$$

$$\epsilon_{\mathrm{DT}} = \frac{P_1\bar{\kappa}_{\mathrm{DT},1} + P_2\bar{\kappa}_{\mathrm{DT},2}}{r_1 + r_2}. \tag{22}$$

Here, $\kappa_{\mathrm{DT},i}$, $i = 1, 2$, denotes the total number of transmissions required at $\mathcal{S}_i$ to transmit $\mathbf{s}_i$ to both $\mathcal{D}_1$ and $\mathcal{D}_2$, which is given as follows:

$$\kappa_{\mathrm{DT},i} = \max\left\{ \min\left\{ k \middle| \sum_{j=1}^{k} \log\left(1 + [\gamma_{ii}]_j\right) > r_i \right\} \right. \\ \left. \min\left\{ k \middle| \sum_{j=1}^{k} \log\left(1 + [\gamma_{ii'}]_j\right) > r_i \right\} \right\} \tag{23}$$

where $i' = i - (-1)^i$, $i = 1, 2$, and $\gamma_{ii'}$ denotes the SNR of the transmission link $\mathcal{S}_i \to \mathcal{D}_{i'}$.

In the high-power regime, all HARQ-IR protocols for both relay-aided and nonrelay-aided transmissions in the WNCBN require two time slots in total to transmit successfully two data packets $\mathbf{s}_1$ and $\mathbf{s}_2$ from $\mathcal{S}_1$ and $\mathcal{S}_2$ to $\mathcal{D}_1$ and $\mathcal{D}_2$, respectively. This means that all the PNC, ANC, and DT schemes achieve the same EDT performance with $\{\delta_{\mathrm{PNC}}, \delta_{\mathrm{ANC}}, \delta_{\mathrm{DT}}\} \to (2/r_1 + r_2)$ and $\{\epsilon_{\mathrm{PNC}}, \epsilon_{\mathrm{ANC}}, \epsilon_{\mathrm{DT}}\} \to \infty$ as $P \to \infty$. Moreover, as shown in Lemma 1 in the following, there is no advantageous scheme in the high-power regime.

*Lemma 1:* If $P$ approaches infinity, then $\epsilon_{\mathrm{PNC}}/\epsilon_{\mathrm{DT}} \to 1$, $\epsilon_{\mathrm{ANC}}/\epsilon_{\mathrm{DT}} \to 1$, and $\epsilon_{\mathrm{PNC}}/\epsilon_{\mathrm{ANC}} \to 1$.

*Proof:* From (12), (13), and (19)–(22), the proof can be straightforwardly obtained. ■

In the low-power regime, the transmission power at all transmitting nodes is assumed equally allocated as $P_1 = P_2 = P_R = P/3$ in the PNC and ANC schemes and $P_1 = P_2 = P/2$ in the DT scheme.[4] Moreover, for simplicity, the data transmission from $\mathcal{S}_1$ and $\mathcal{S}_2$ to $\mathcal{D}_1$ and $\mathcal{D}_2$, respectively, is assumed carried out at the same data rate, i.e., $r_1 = r_2 = R$.

First, let us derive the EDT of the HARQ-IR protocol in the WNCBN with the DT scheme. We have the following finding.

*Lemma 2:* If $P$ approaches 0, then the ED and EB of the HARQ-IR protocol with the DT scheme are approximated by $\delta_{\mathrm{DT},0}$ and $\epsilon_{\mathrm{DT},0}$, respectively, where

$$\delta_{\mathrm{DT},0} = \frac{\ln 2}{P}\left(\max\left\{d^{\nu}_{S_1D_1}, d^{\nu}_{S_1D_2}\right\} + \max\left\{d^{\nu}_{S_2D_1}, d^{\nu}_{S_2D_2}\right\}\right) \tag{24}$$

$$\epsilon_{\mathrm{DT},0} = \frac{\ln 2}{2}\left(\max\left\{d^{\nu}_{S_1D_1}, d^{\nu}_{S_1D_2}\right\} + \max\left\{d^{\nu}_{S_2D_1}, d^{\nu}_{S_2D_2}\right\}\right). \tag{25}$$

*Proof:* See Appendix A. ■

Investigating the EDT of the HARQ-IR protocols with PNC and ANC schemes in the low-power regime, we have the following findings.

*Lemma 3:* If $P$ approaches 0, then the ED and EB of the HARQ-IR protocol with the PNC scheme are approximated by $\delta_{\mathrm{PNC},0}$ and $\epsilon_{\mathrm{PNC},0}$, respectively, where

$$\delta_{\mathrm{PNC},0} = \frac{3\ln 2}{2P}\left(\max\left\{d^{\nu}_{S_1D_1}, d^{\nu}_{S_2D_2}\right\} + \max\left\{d^{\nu}_{RD_1}, d^{\nu}_{RD_2}\right\}\right) \tag{26}$$

$$\epsilon_{\mathrm{PNC},0} = \frac{\ln 2}{2}\left(d^{\nu}_{S_1D_1} + d^{\nu}_{S_2D_2} + \max\left\{d^{\nu}_{RD_1}, d^{\nu}_{RD_2}\right\}\right). \tag{27}$$

*Proof:* See Appendix B. ■

*Lemma 4:* If $P$ approaches 0, then the ED and EB of the HARQ-IR protocol with the ANC scheme are approximated by $\delta_{\mathrm{ANC},0}$ and $\epsilon_{\mathrm{ANC},0}$, respectively, where

$$\delta_{\mathrm{ANC},0} = \frac{9\ln 2}{P^2}\max\left\{d^{\nu}_{S_1R}d^{\nu}_{RD_2}, d^{\nu}_{S_2R}d^{\nu}_{RD_1}\right\} \tag{28}$$

$$\epsilon_{\mathrm{ANC},0} = \frac{9\ln 2}{4P}\left(d^{\nu}_{S_1R}d^{\nu}_{RD_2} + d^{\nu}_{S_2R}d^{\nu}_{RD_1}\right). \tag{29}$$

*Proof:* See Appendix C. ■

From the given lemmas, we have the following observations in the low-power regime.

*(O1) Energy inefficiency with ANC*: It is shown in (29) that $\epsilon_{\mathrm{ANC},0}$ increases as $P$ decreases. This means that the ANC

[3] Note that, in the DT scheme, $P_R = 0$ and $\rho_1 + \rho_2 = 1$.

[4] It is noted that the equal power allocation is not optimal in general. However, as $P \to 0$, it is reasonable to assume the equal power allocation at all transmitting nodes.

scheme is not energy efficient when compared with the DT and PNC schemes for the HARQ-IR protocol in the WNCBN.

*(O2) Higher energy efficiency with PNC when the relay node is located far from source nodes*: In fact, when $\mathcal{R}$ is far from $\mathcal{S}_1$ and $\mathcal{S}_2$, we have $\{d^{\nu}_{RD_1}, d^{\nu}_{RD_2}\} \ll \{d^{\nu}_{S_1D_1}, d^{\nu}_{S_2D_2}\}$. Thus, $d^{\nu}_{S_1D_1}+d^{\nu}_{S_2D_2}+\max\{d^{\nu}_{RD_1}, d^{\nu}_{RD_2}\} \approx d^{\nu}_{S_1D_1}+d^{\nu}_{S_2D_2}$. Accordingly, from (25) and (27), it can be shown that $\epsilon_{\mathrm{PNC},0} < \epsilon_{\mathrm{DT},0}$, which means the HARQ-IR protocol with the PNC scheme is more energy efficient than the HARQ-IR protocol with the DT scheme.

*(O3) Higher energy efficiency with DT over PNC when relay node is located nearby source nodes*: In this scenario, we can approximate $\{d^{\nu}_{RD_1}, d^{\nu}_{RD_2}\} \gtrapprox \{d^{\nu}_{S_1D_1}, d^{\nu}_{S_2D_2}\}$. Thus, from (25) and (27), we have $\epsilon_{\mathrm{PNC},0} > \epsilon_{\mathrm{DT},0}$. This means that the DT scheme is more energy efficient than the PNC scheme for the HARQ-IR protocol in the WNCBN. In other words, there is no advantage of employing the relay when the relay is in the neighborhood of the sources.

## V. Relay Positioning in Wireless-Network-Coded Butterfly Networks

In WNCBNs, the data transmissions from two source nodes to two destination nodes are carried out via a relay node operating under either PNC or ANC protocols. Taking into account the EDT performance, the location of the relay may have a considerable impact on the energy efficiency in the WNCBNs. However, optimizing RP in terms of delay and energy consumption has attracted little attention in previous work, e.g., [22]–[25]. In this paper, based on the derived EDT for HARQ-IR protocols with PNC and ANC, we propose algorithms for solving the RP optimization problem subject to location and power constraints in WNCBNs.[5]

The problem relates to how to position the relay node to minimize either the total delay or the total energy consumption of all the multicast transmissions from two source nodes to two destination nodes. As shown in Fig. 1, the relay location can be determined through the distance between $\mathcal{S}_1$ and $\mathcal{R}$ (i.e., $d_{S_1R}$), and the angle $\widehat{\mathcal{D}_1\mathcal{S}_1\mathcal{R}}$ (i.e., $\alpha_R$). Based on $d_{S_1R}$ and $\alpha_R$, we can easily evaluate the distance from $\mathcal{R}$ to $\mathcal{S}_2$, $\mathcal{D}_1$, and $\mathcal{D}_2$, as

$$d_{S_2R} = \sqrt{d^2_{S_1S_2} + d^2_{S_1R} - 2d_{S_1S_2}d_{S_1R}\cos(\alpha_1 - \alpha_R)} \quad (30)$$

$$d_{RD_1} = \sqrt{d^2_{S_1D_1} + d^2_{S_1R} - 2d_{S_1D_1}d_{S_1R}\cos\alpha_R} \quad (31)$$

$$d_{RD_2} = \sqrt{d^2_{S_2D_2} + d^2_{S_2R} - 2d_{S_2D_2}d_{S_2R}\cos\beta_R}. \quad (32)$$

Here, $\beta_R$ denotes the angle $\widehat{\mathcal{D}_2\mathcal{S}_2\mathcal{R}}$, which can be computed by

$$\beta_R = \alpha_2 - \sin^{-1}\left(\frac{d_{S_1R}}{d_{S_2R}}\sin(\alpha_1 - \alpha_R)\right). \quad (33)$$

[5]In this paper, with fixed location of the source and destination nodes, we determine the best relay location with respect to different HARQ-IR protocols. This is useful for the system where the mobile users play the role as the relay nodes; thus, the user having the best relay location would be selected for the relay communications.

Let $\{d^*_{S_1R,\delta_{\mathrm{PNC}}}, \alpha^*_{S_1R,\delta_{\mathrm{PNC}}}\}$, $\{d^*_{S_1R,\delta_{\mathrm{ANC}}}, \alpha_{R,\delta^*_{\mathrm{ANC}}}\}$, $\{d^*_{S_1R,\epsilon_{\mathrm{PNC}}}, \alpha^*_{R,\epsilon_{\mathrm{PNC}}}\}$, and $\{d^*_{S_1R,\epsilon_{\mathrm{ANC}}}, \alpha^*_{R,\epsilon_{\mathrm{ANC}}}\}$ denote the optimized positioning parameters for the relay location using PNC and ANC protocols subject to minimizing $\delta_{\mathrm{PNC}}$, $\delta_{\mathrm{ANC}}$, $\epsilon_{\mathrm{PNC}}$, and $\epsilon_{\mathrm{ANC}}$, respectively. The RP optimization problem is therefore expressed as

$$\left\{d^*_{S_1R,\delta_{\mathrm{PNC}}}, \alpha^*_{R,\delta_{\mathrm{PNC}}}\right\} = \arg\min_{d_{S_1R},\alpha_R} \delta_{\mathrm{PNC}} \quad (34)$$

$$\left\{d^*_{S_1R,\delta_{\mathrm{ANC}}}, \alpha^*_{R,\delta_{\mathrm{ANC}}}\right\} = \arg\min_{d_{S_1R},\alpha_R} \delta_{\mathrm{ANC}} \quad (35)$$

$$\left\{d^*_{S_1R,\epsilon_{\mathrm{PNC}}}, \alpha^*_{R,\epsilon_{\mathrm{PNC}}}\right\} = \arg\min_{d_{S_1R},\alpha_R} \epsilon_{\mathrm{PNC}} \quad (36)$$

$$\left\{d^*_{S_1R,\epsilon_{\mathrm{ANC}}}, \alpha^*_{R,\epsilon_{\mathrm{ANC}}}\right\} = \arg\min_{d_{S_1R},\alpha_R} \epsilon_{\mathrm{ANC}} \quad (37)$$

where $\delta_{\mathrm{PNC}}$, $\delta_{\mathrm{ANC}}$, $\epsilon_{\mathrm{PNC}}$, and $\epsilon_{\mathrm{ANC}}$ are generally given by (12), (19), (13), and (20), respectively.[6] Given the fixed location of the source and destination nodes (see Fig. 1), $d_{S_1R}$ and $\alpha_R$ are bounded by the following ranges:

$$0 < d_{S_1R} < \max\left\{\sqrt{d^2_{S_1D_1} + d^2_{S_1S_2} - 2d_{S_1D_1}d_{S_1S_2}\cos\alpha_1}\right.$$
$$\left.\sqrt{d^2_{S_1D_1} + d^2_{D_1D_2} - 2d_{S_1D_1}d_{D_1D_2}\cos\alpha_4}\right\} \quad (38)$$

$$0 < \alpha_R < \alpha_1. \quad (39)$$

We have the following observations.

*(O4) ANC-based relay can be nearly located at the same location for minimizing both the delay and energy*: In fact, given a compact set $\mathbb{S}$, it is noted that $\arg\min_{x_1,x_2\in\mathbb{S}} \max\{f(x_1),f(x_2)\} \approx \arg\min_{x_1,x_2\in\mathbb{S}} f(x_1)+f(x_2)$. Thus, from (19) and (20), we can approximate $\arg\min_{d_{S_1R},\alpha_R} \delta_{\mathrm{ANC}} \approx \arg\min_{d_{S_1R},\alpha_R} \epsilon_{\mathrm{ANC}}$, which means $\{d^*_{S_1R,\delta_{\mathrm{ANC}}}, \alpha^*_{R,\delta_{\mathrm{ANC}}}\} \approx \{d^*_{S_1R,\epsilon_{\mathrm{ANC}}}, \alpha^*_{R,\epsilon_{\mathrm{ANC}}}\}$.

*(O5) Perspective transformation for a general setting of the node positions in an irregular quadrilateral*: We can realize a spatial transformation to map the nodes in a quadrilateral to the nodes in a rectangle [35]. Then, we find the optimal relay position in the rectangular region (namely, virtual relay positions) for minimizing either delay or energy. The real relay position for the irregular quadrilateral node setting can be found by an inverse mapping. Specifically, a perspective transformation or projective nonaffine mapping with bilinear interpolation can be used to map a quadrilateral to a rectangle as follows. Given four 2-D points $A$, $B$, $C$, and $D$ of a quadrilateral located at $(x_A, y_A)$, $(x_B, y_B)$, $(x_C, y_C)$, and $(x_D, y_D)$, and four 2-D points $A'$, $B'$, $C'$, and $D'$ of a rectangle located at $(x_{A'}, y_{A'})$, $(x_{B'}, y_{B'})$, $(x_{C'}, y_{C'})$, and $(x_{D'}, y_{D'})$, we can map $\{A, B, C, D\}$ to $\{A', B', C', D'\}$ by finding a $4 \times 4$ mapping matrix $\mathbf{M}$, i.e., [35]

$$\begin{pmatrix} 1 & x_A & y_A & x_Ay_A \\ 1 & x_B & y_B & x_By_B \\ 1 & x_C & y_C & x_Cy_C \\ 1 & x_D & y_D & x_Dy_D \end{pmatrix} \mathbf{M} = \begin{pmatrix} 1 & x_{A'} & y_{A'} & x_{A'}y_{A'} \\ 1 & x_{B'} & y_{B'} & x_{B'}y_{B'} \\ 1 & x_{C'} & y_{C'} & x_{C'}y_{C'} \\ 1 & x_{D'} & y_{D'} & x_{D'}y_{D'} \end{pmatrix}.$$

[6]It is noted that, in the low-power regime, $\delta_{\mathrm{PNC}} \approx \delta_{\mathrm{PNC},0}$, $\delta_{\mathrm{ANC}} \approx \delta_{\mathrm{ANC},0}$, $\epsilon_{\mathrm{PNC}} \approx \epsilon_{\mathrm{PNC},0}$, and $\epsilon_{\mathrm{ANC}} \approx \epsilon_{\mathrm{ANC},0}$, which are determined by (26)–(29), respectively.

According to observation (O5), for simplicity, let us investigate a specific scenario where $\alpha_1 = \alpha_2 = \alpha_3 = \alpha_4 = \pi/2$, $d_{S_1D_1} = d_{S_2D_2}$, and $d_{S_1S_2} = d_{D_1D_2}$. The search range of the relay position given by (38) and (39) can be rewritten as

$$0 < d_{S_1R} < \sqrt{d_{S_1D_1}^2 + d_{S_1S_2}^2} \tag{40}$$

$$0 < \alpha_R < \frac{\pi}{2}. \tag{41}$$

With the total power constraint $P$ and different power allocation at $\mathcal{S}_1$ and $\mathcal{S}_2$, there are three typical cases based on the relationship between $P_1$ and $P_2$, which are described as follows.

### A. $P_1 = P_2$

Due to the equal power allocation at $\mathcal{S}_1$ and $\mathcal{S}_2$, $\mathcal{R}$ is located on the median line between the pair nodes $\{\mathcal{S}_1, \mathcal{D}_1\}$ and $\{\mathcal{S}_2, \mathcal{D}_2\}$. Let us denote $d_R = \sqrt{d_{S_1R}^2 - d_{S_1S_2}^2/4}$. The RP optimization in (34)–(37) can be determined through

$$d_{R,\delta_X}^* = \arg \min_{0<d_R<d_{S_1D_1}} \delta_X \tag{42}$$

$$d_{R,\epsilon_X}^* = \arg \min_{0<d_R<d_{S_1D_1}} \epsilon_X \tag{43}$$

where $X \in \{\text{PNC}, \text{ANC}\}$. Then, we can determine $\{d_{S_1R,\delta_X}^*, \alpha_{R,\delta_X}^*\}$, and $\{d_{S_1R,\epsilon_X}^* \alpha_{1R,\epsilon_X}^*\}$ as

$$d_{S_1R,\delta_X}^* = \sqrt{d_{R,\delta_X}^{*2} + \frac{d_{S_1S_2}^2}{4}}, \quad \alpha_{R,\delta_X}^* = \tan^{-1}\left(\frac{d_{S_1S_2}}{2d_{R,\delta_X}^*}\right) \tag{44}$$

$$d_{S_1R,\epsilon_X}^* = \sqrt{d_{R,\epsilon_X}^{*2} + \frac{d_{S_1S_2}^2}{4}}, \quad \alpha_{R,\epsilon_X}^* = \tan^{-1}\left(\frac{d_{S_1S_2}}{2d_{R,\epsilon_X}^*}\right). \tag{45}$$

It can be observed that the optimized positioning search algorithms using (42)–(45) require lower complexity processing than an exhaustive search of all available relay positions in the whole region encompassing the four source and destination nodes with the constraints of (40) and (41).

### B. $P_1 > P_2$

In this scenario, $\mathcal{R}$ is located in the neighborhood region of the pair node $\{\mathcal{S}_2, \mathcal{D}_2\}$. Thus, the search range for the optimized relay location in (40) and (41) can be limited by two regions defined as follows:

$$\text{Region (I)}: \begin{cases} \tan^{-1}\left(\frac{d_{S_1S_2}}{2d_{S_1D_1}}\right) < \alpha_R < \tan^{-1}\left(\frac{d_{S_1S_2}}{d_{S_1D_1}}\right) \\ \frac{d_{S_1S_2}}{2\sin\alpha_R} < d_{S_1R} < \frac{d_{S_1D_1}}{\cos\alpha_R} \end{cases} \tag{46}$$

$$\text{Region (II)}: \begin{cases} \tan^{-1}\left(\frac{d_{S_1S_2}}{d_{S_1D_1}}\right) < \alpha_R < \frac{\pi}{2} \\ \frac{d_{S_1S_2}}{2\sin\alpha_R} < d_{S_1R} < \frac{d_{S_1S_2}}{\sin\alpha_R}. \end{cases} \tag{47}$$

With various relay positions in regions (I) and (II), we can then determine the optimized relay location $\{d_{S_1R,\delta_X}^*, \alpha_{R,\delta_X}^*\}$ and $\{d_{S_1R,\epsilon_X}^*, \alpha_{R,\epsilon_X}^*\}$, $X \in \{\text{PNC}, \text{ANC}\}$, subject to minimizing either $\delta_X$ or $\epsilon_X$ as in (34)–(37). Regarding the search range in the context of $P_1 > P_2$, it can be observed that the search regions (I) and (II) are narrower than the region determined by (40) and (41); thus, the complexity of the search for the optimized relay location is reduced.

### C. $P_1 < P_2$

Similarly, in this scenario, $\mathcal{R}$ is located near the two nodes $\mathcal{S}_1$ and $\mathcal{D}_1$. The search range for the optimized relay location in (40) and (41) can be thus limited by two regions defined as follows:

$$\text{Region (III)}: \begin{cases} 0 < \alpha_R < \tan^{-1}\left(\frac{d_{S_1S_2}}{2d_{S_1D_1}}\right) \\ 0 < d_{S_1R} < \frac{d_{S_1D_1}}{\cos\alpha_R} \end{cases} \tag{48}$$

$$\text{Region (IV)}: \begin{cases} \tan^{-1}\left(\frac{d_{S_1S_2}}{2d_{S_1D_1}}\right) < \alpha_R < \frac{\pi}{2} \\ 0 < d_{S_1R} < \frac{d_{S_1S_2}}{2\sin\alpha_R}. \end{cases} \tag{49}$$

Then, we can determine the optimized relay location $\{d_{S_1R,\delta_X}^*, \alpha_{R,\delta_X}^*\}$ and $\{d_{S_1R,\epsilon_X}^*, \alpha_{R,\epsilon_X}^*\}$, $X \in \{\text{PNC}, \text{ANC}\}$, in regions (III) and (IV) to minimize either $\delta_X$ or $\epsilon_X$. Additionally, it can be observed that the search regions (III) and (IV) for the scenario $P_1 < P_2$ are also narrower than the region determined by (40) and (41), and again a low-complexity search algorithm is achieved.

## VI. Numerical Results

Here, we present the numerical results of the EDT and relay location optimization in a WNCBN using various HARQ-IR protocols when all channels experience quasi-static Rayleigh block fading. A symmetric network structure is considered with $d_{S_1D_1} = d_{S_2D_2}$, $d_{S_1S_2} = d_{D_1D_2}$, and $\alpha_1 = \alpha_2 = \alpha_3 = \alpha_4 = \pi/2$. The data transmission from $\mathcal{S}_1$ and $\mathcal{S}_2$ to $\mathcal{D}_1$ and $\mathcal{D}_2$ is carried out at the same data rate (i.e., $r_1 = r_2 = R$) via either HARQ-IR with DT or PNC or ANC schemes. The path-loss exponent between a pair of transceiver nodes is assumed $\nu = 3$.

Let us first investigate the EDT in the WNCBN with HARQ-IR protocols with DT, PNC, and ANC. As shown in Fig. 2, the EDT curves are plotted for the three HARQ-IR protocols. The data rate at $\mathcal{S}_1$ and $\mathcal{S}_2$ is 5 b/s. The relay $\mathcal{R}$ is assumed located at the center of the network, where the distances and angles are set as $d_{S_1D_1} = d_{S_2D_2} = 1$, $d_{S_1S_2} = d_{D_1D_2} = 1/\sqrt{3}$, $\alpha_R = \pi/6$, and $d_{S_1R} = d_{S_2R} = d_{RD_1} = d_{RD_2} = d_{S_1D_1}/2/\cos\alpha_R$. The transmission power at $\mathcal{S}_1$, $\mathcal{S}_2$, and $\mathcal{R}$ is assumed equally allocated. It can be seen that the PNC scheme is more energy efficient than both the ANC and DT schemes. In fact, using the HARQ-IR protocol with PNC, $\mathcal{R}$ can help $\mathcal{S}_1$ and $\mathcal{S}_2$ retransmit the corrupted combined packets to both $\mathcal{D}_1$ and $\mathcal{D}_2$. Using the HARQ-IR protocol with the ANC scheme, $\mathcal{S}_1$ and $\mathcal{S}_2$ are required to retransmit the corrupted packets to $\mathcal{R}$, then $\mathcal{R}$ combines the received packets and broadcasts the new combined packets to both $\mathcal{D}_1$ and $\mathcal{D}_2$. Using the DT scheme, there is no relay to assist $\mathcal{S}_1$ and $\mathcal{S}_2$ retransmit the corrupted combined packets to both $\mathcal{D}_1$ and $\mathcal{D}_2$. Due to the long distances

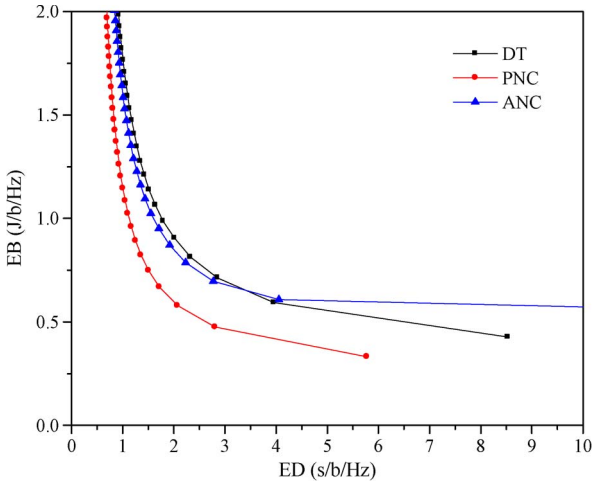


Fig. 2. EDT of various HARQ-IR protocols in WNCBN with $R = 5$ b/s, $d_{S_1D_1} = d_{S_2D_2} = 1$, $d_{S_1S_2} = d_{D_1D_2} = 1/\sqrt{3}$, $\alpha_R = \pi/6$, and $d_{S_1R} = d_{S_2R} = d_{RD_1} = d_{RD_2} = d_{S_1D_1}/2/\cos\alpha_R$.

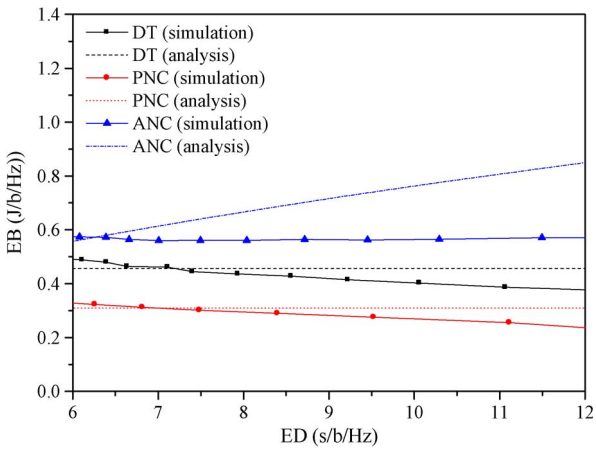


Fig. 3. EDT of various HARQ-IR protocols in the low-power regime with $R = 5$ b/s, $d_{S_1D_1} = d_{S_2D_2} = 1$, $d_{S_1S_2} = d_{D_1D_2} = 1/\sqrt{3}$, $\alpha_R = \pi/6$, and $d_{S_1R} = d_{S_2R} = d_{RD_1} = d_{RD_2} = d_{S_1D_1}/2/\cos\alpha_R$.

from $\mathcal{S}_1$ to $\mathcal{D}_2$ and from $\mathcal{S}_2$ to $\mathcal{D}_1$, the DT scheme is shown to be less energy efficient than the PNC scheme. However, the EDT of the DT scheme is better than that of the ANC scheme since a recombination process is required at $\mathcal{R}$ in the ANC scheme, which means more energy consumption at $\mathcal{R}$. This confirms the statements in observations (O1) and (O2) regarding a lower energy efficiency of the ANC scheme and a higher energy efficiency of the PNC scheme over the DT scheme when the relay node is located far from the source nodes.

Fig. 3 shows the EDT curves for the three HARQ-IR protocols in the low-power regime. The data rates and position of all nodes are set as in Fig. 2. Moreover, the transmission power at $\mathcal{S}_1$, $\mathcal{S}_2$, and $\mathcal{R}$ is assumed equally allocated. In Fig. 3, both simulation and analytical results are shown. Similarly, in the low-power regime, it is observed that the PNC scheme achieves a higher energy efficiency, whereas a lower energy efficiency with the ANC scheme over the DT scheme. Additionally, the simulation results are shown to be approximated by the analytical approximation results in Section IV. This also confirms the statements in observations (O1) and (O2) regarding the higher

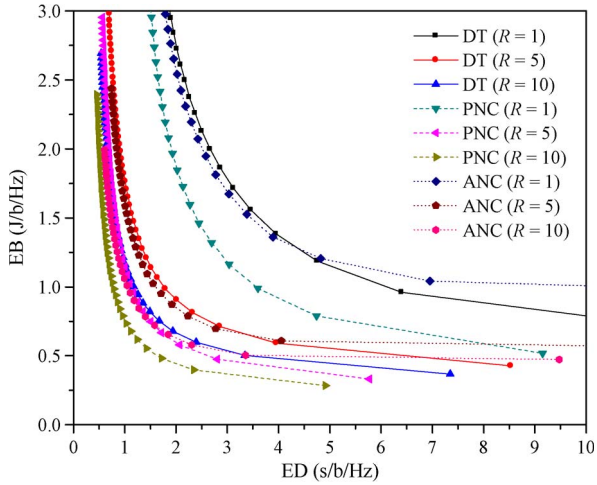


Fig. 4. Comparison of EDTs of various HARQ-IR protocols in WNCBN with various data rates and $d_{S_1D_1} = d_{S_2D_2} = 1$, $d_{S_1S_2} = d_{D_1D_2} = 1/\sqrt{3}$, $\alpha_R = \pi/6$, and $d_{S_1R} = d_{S_2R} = d_{RD_1} = d_{RD_2} = d_{S_1D_1}/2/\cos\alpha_R$.

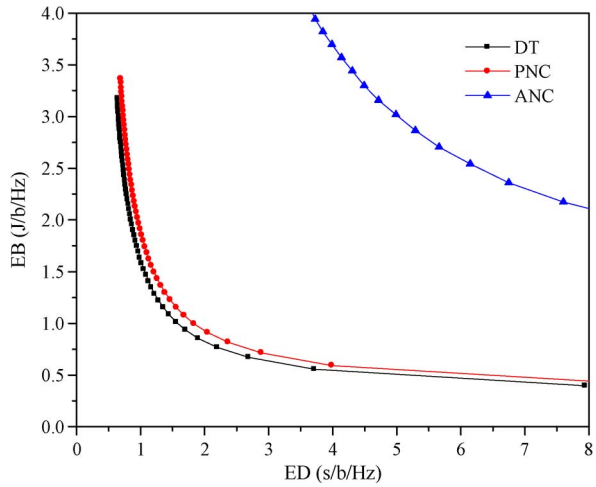


Fig. 5. EDTs of various HARQ-IR protocols in the WNCBN for the scenario when relay near sources with $R = 5$ b/s, $d_{S_1D_1} = d_{S_2D_2} = 1$, $d_{S_1S_2} = d_{D_1D_2} = 1/2$, $\alpha_R = \pi/10$, and $d_{S_1R} = 1/8$.

energy efficiency with the PNC scheme and the lower energy efficiency with the ANC scheme in the low-power regime.

The impact of data rate on the EDT performance is shown in Fig. 4, where the data rates at $\mathcal{S}_1$ and $\mathcal{S}_2$ are assumed equal and vary in the ranges {1, 5, 10} b/s. The position of all nodes is set as in Fig. 2, and the transmission power at $\mathcal{S}_1$, $\mathcal{S}_2$, and $\mathcal{R}$ is again assumed equally allocated. Similarly, we can observe that the best performance is achieved with the PNC scheme at all data rates, and in addition, the ANC scheme is always less energy efficient than both the PNC and DT schemes. This comparison of energy efficiency again verifies the statements in observations (O1) and (O2) at all data rates. Moreover, it is shown in Fig. 4 that an improved EDT is achieved for all HARQ-IR protocols as the data rate increases.

Taking into account the practical scenario where the relay is not always located at the center of the network, Figs. 5 and 6 plot the EDT curves of various HARQ-IR protocols in the WNCBN with respect to different relay positions. Specifically, Fig. 5 corresponds to the scenario when the relay is

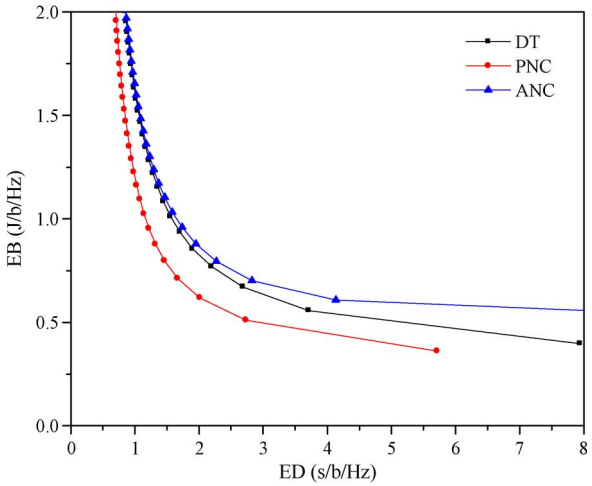


Fig. 6. EDTs of various HARQ-IR protocols in the WNCBN for the scenario when relay near destinations with $R = 5$ b/s, $d_{S_1D_1} = d_{S_2D_2} = 1$, $d_{S_1S_2} = d_{D_1D_2} = 1/2$, $\alpha_R = \pi/10$, and $d_{S_1R} = 7/8$.

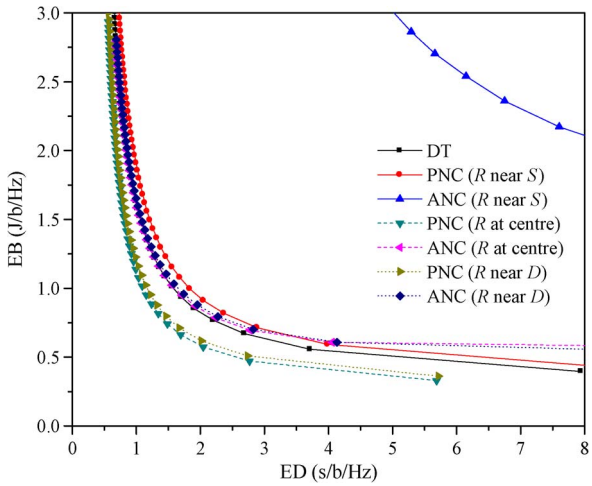


Fig. 7. Comparison of EDTs of various HARQ-IR protocols in the WNCBN with $R = 5$ b/s, $d_{S_1D_1} = d_{S_2D_2} = 1$, $d_{S_1S_2} = d_{D_1D_2} = 1/2$, and various relay positions.

near the sources ($\alpha_R = \pi/10$, $d_{S_1R} = 1/8$), and Fig. 6 is related to the scenario when the relay is near the destinations ($\alpha_R = \pi/10$, $d_{S_1R} = 7/8$). The distances between the sources and destinations are fixed as $d_{S_1D_1} = d_{S_2D_2} = 1$ and $d_{S_1S_2} = d_{D_1D_2} = 1/2$. The transmission power at $\mathcal{S}_1$, $\mathcal{S}_2$, and $\mathcal{R}$ is also assumed equally allocated, and the data rate is assumed 5 b/s. As shown in Fig. 5, the DT scheme is shown to be the most energy-efficient scheme compared with both the PNC and ANC schemes when the relay is in the neighborhood of the sources. This confirms the statement in observation (O3) in relation to the higher energy efficiency of the DT scheme when the relay is located near the sources. In fact, it can be intuitively observed that the relay plays the same role as the sources if the relay is located near the sources, which means the use of the relay in the PNC and ANC schemes is not as energy efficient compared with the DT scheme, although the relay can be used in this case to increase the transmit diversity order. For the scenario when the relay is near the destinations (see Fig. 6), the relay is shown to be energy efficient with the PNC scheme, whereas with the ANC scheme, it is seen to be less energy efficient. This again verifies the statements in observations (O1) and (O2), which are similar to the scenario when the relay is located at the center of the network.

The impact of relay positions on the EDT performance is summarized in Fig. 7 where three typical relay positions are taken into consideration, including the scenarios when the relay is located either near the sources or near the destinations or at the center of the network. The data rate is set as 5 b/s, and the transmission power at all nodes is equally allocated. For the first two scenarios, the EDT curves are similar to those in Figs. 5 and 6 with similar settings of the node positions. For the third scenario, the relay position is determined by $\alpha_R = \arctan(d_{S_1S_2}/d_{S_1D_1})$ and $d_{S_1R} = \sqrt{d_{S_1D_1}^2 + d_{S_1S_2}^2}/2$. It is shown in Fig. 7 that the most energy-efficient scheme is the PNC scheme with respect to the scenario when the relay is located at the center of the network. Further, applying the ANC scheme to the scenario when the relay is near the sources results in the worst EDT performance.

Investigating the optimization of RP for minimum ED in WNCBNs, Figs. 8 and 9 sequentially plot the optimized relay locations as a function of power allocation when HARQ-IR protocols are employed with PNC and ANC for various scenarios of power allocations at the source nodes. The EDT corresponding to the optimized relay locations is also included to compare the energy efficiency of the two HARQ-IR protocols. Fig. 8 considers the scenario of equal power allocation (i.e., $P_1 = P_2$), whereas Fig. 9 investigates the scenario of unequal power allocation[7] $P_1 = nP_2, n > 1$. The bisection search method is applied to find the optimal relay position in the search region. We assume that $R = 5$ b/s, $P_{\text{total}} = P_1 + P_2 + P_R = 5$ W, $d_{S_1D_1} = d_{S_2D_2} = 1$, and $d_{S_1S_2} = d_{D_1D_2} = 1/2$. The optimized relay locations in Figs. 8 and 9 are determined through $d_{S_1R}$ and $\alpha_R$ using the proposed algorithms in Section IV for different power allocations. It is shown in Figs. 8(c) and 9(c) that the PNC scheme is more energy efficient than the ANC scheme, although the EDT curves have different shapes as $n$ varies due to the impact of relay position (see Fig. 7). This again validates the effectiveness of the PNC scheme over the ANC scheme for all power allocations. Additionally, it can be observed in Fig. 8 for the scenario $P_1 = P_2$ that, as $P_1$ and $P_2$ increase, the optimized location of both the ANC-based and PNC-based $\mathcal{R}$ move from the region near $\mathcal{S}_1$ and $\mathcal{S}_2$ to the region near $\mathcal{D}_1$ and $\mathcal{D}_2$. However, when $P_1$ and $P_2$ are small, the ANC-based $\mathcal{R}$ is closer to $\mathcal{S}_1$ and $\mathcal{S}_2$ than the PNC-based $\mathcal{R}$. For the case $P_1 = nP_2$ in Fig. 9, as $n$ increases, the optimized location of the ANC-based $\mathcal{R}$ is closer to $\mathcal{S}_2$, whereas that of the PNC-based $\mathcal{R}$ is farther away from $\mathcal{D}_2$.

Considering the total energy consumption in the optimization of RP, Figs. 10 and 11 sequentially plot the optimized relay locations as a function of power allocation at the source nodes using HARQ-IR protocols with PNC and ANC. Moreover, the EDT corresponding to the optimized relay locations for minimum EB is included to compare the energy efficiency of the two HARQ-IR protocols. The power allocations at the

[7]Note that the RP for the scenario $P_2 = nP_1$ can be similarly observed to be symmetric with that for the scenario $P_1 = nP_2$ and is thus omitted for brevity.

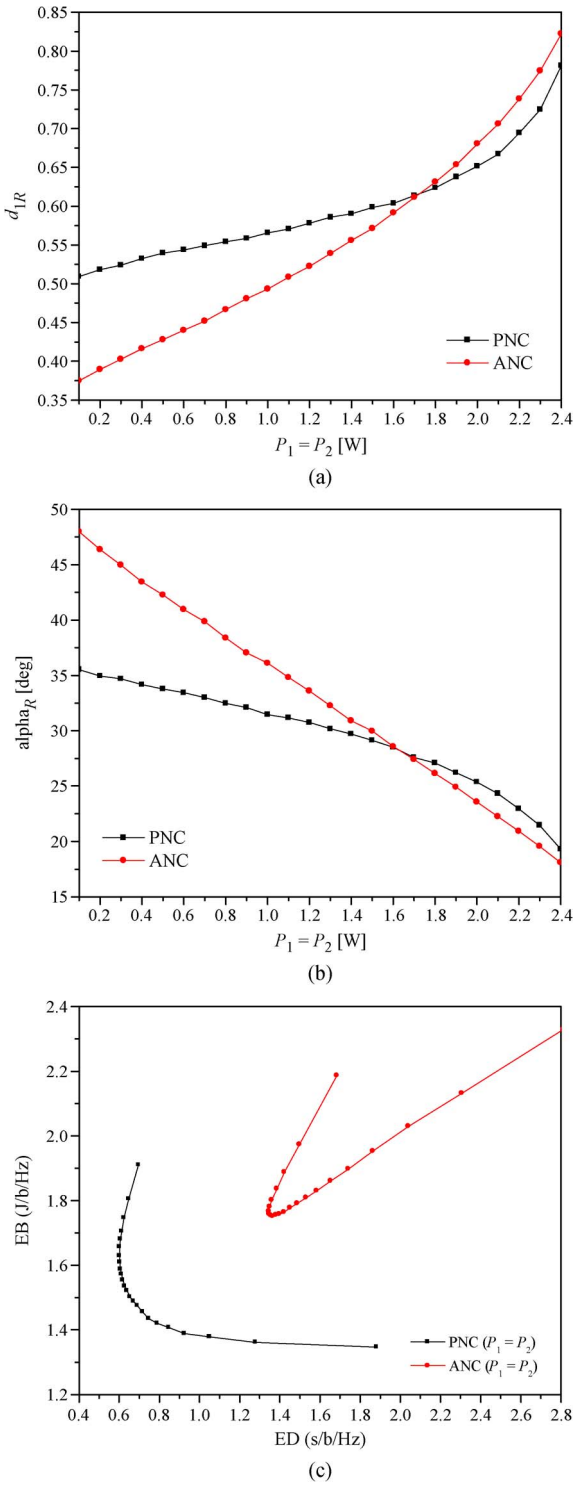


Fig. 8. Optimization of relay location subject to minimizing ED with $R = 5$ b/s, $P_{\text{total}} = 5$ W, $P_1 = P_2$, $d_{S_1D_1} = d_{S_2D_2} = 1$, and $d_{S_1S_2} = d_{D_1D_2} = 1/2$. (a) $d_{S_1R}$. (b) $\alpha_R$. (c) EDT.

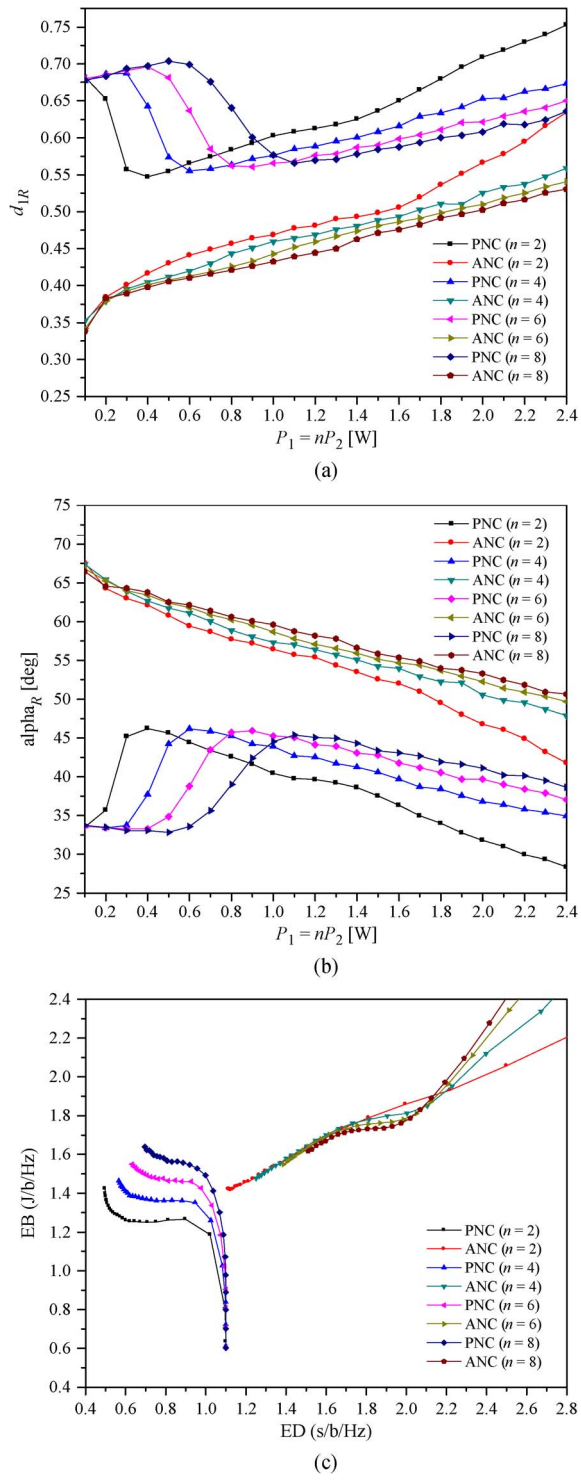


Fig. 9. Optimization of relay location subject to minimizing ED with $R = 5$ b/s, $P_{\text{total}} = 5$ W, $P_1 = nP_2$, $d_{S_1D_1} = d_{S_2D_2} = 1$, and $d_{S_1S_2} = d_{D_1D_2} = 1/2$. (a) $d_{S_1R}$. (b) $\alpha_R$. (c) EDT.

two source nodes are similarly assumed as in Figs. 8 and 9. We also assume that $R = 5$ b/s, $P_{\text{total}} = P_1 + P_2 + P_R = 5$ W, $d_{S_1D_1} = d_{S_2D_2} = 1$, and $d_{S_1S_2} = d_{D_1D_2} = 1/2$. Using the proposed algorithms in Section IV for different power allocations, the optimized relay locations for minimum EB are determined. Again, Figs. 10(c) and 11(c) confirm the higher energy efficiency of the PNC scheme over the ANC scheme, although the EDT curves also have different shapes due to the impact of relay position. Additionally, in Fig. 10 for the scenario $P_1 = P_2$, it can be observed that, as $P_1$ and $P_2$ increase, the optimized location of the ANC-based $\mathcal{R}$ moves from the region near $\mathcal{S}_1$ and $\mathcal{S}_2$ to the region near $\mathcal{D}_1$ and $\mathcal{D}_2$, whereas that of the PNC-based $\mathcal{R}$ moves in the reverse direction. For the case $P_1 = nP_2$ in Fig. 11, similar to Fig. 9, it is shown that, as

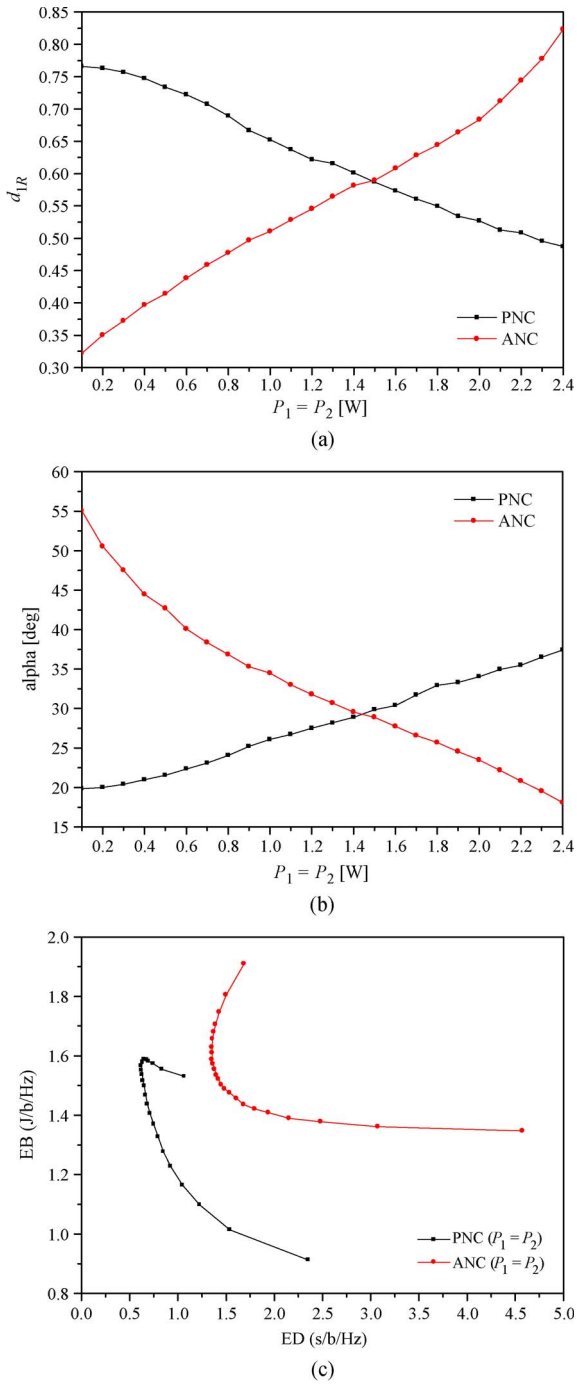


Fig. 10. Optimization of relay location subject to minimizing EB with $R = 5$ b/s, $P_{\text{total}} = 5$ W, $P_1 = P_2$, $d_{S_1D_1} = d_{S_2D_2} = 1$, and $d_{S_1S_2} = d_{D_1D_2} = 1/2$. (a) $d_{S_1R}$. (b) $\alpha_R$. (c) EDT.

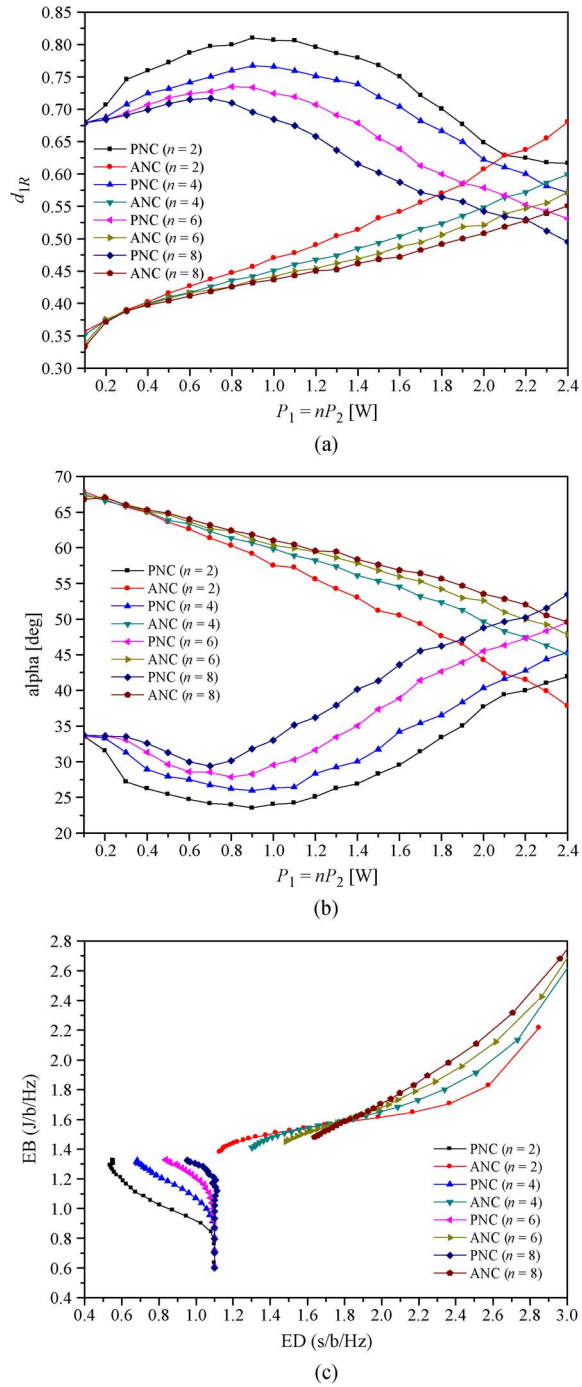


Fig. 11. Optimization of relay location subject to minimizing EB with $R = 5$ b/s, $P_{\text{total}} = 5$ W, $P_1 = nP_2$, $d_{S_1D_1} = d_{S_2D_2} = 1$, and $d_{S_1S_2} = d_{D_1D_2} = 1/2$. (a) $d_{S_1R}$. (b) $\alpha_R$. (c) EDT.

$n$ increases, the ANC-based $\mathcal{R}$ should be closer to $\mathcal{S}_2$, whereas that of the PNC-based $\mathcal{R}$ should be farther away from $\mathcal{D}_2$.

Regarding the optimized relay locations, for clarity, Figs. 12 and 13 show detailed examples of relay locations for either minimum ED or EB for three specific scenarios of power allocations, including $P_1 = P_2$ and $P_1 = 2P_2$. Let us first consider the RP objective of minimum ED. It can be observed in Fig. 12(a) that the ANC-based $\mathcal{R}$ should be located nearer to $\mathcal{D}_1$ and $\mathcal{D}_2$ than the PNC-based $\mathcal{R}$ if $P_1 = P_2 \gg P_R$. In the case $P_1 = P_2 \ll P_R$, the ANC-based $\mathcal{R}$ should remain much closer to $\mathcal{S}_1$ and $\mathcal{S}_2$ compared with the PNC-based $\mathcal{R}$. Considering the scenario when $P_1 > P_2$, as shown in Fig. 12(b), the ANC-based $\mathcal{R}$ should be positioned near $\mathcal{S}_2$, whereas the PNC-based $\mathcal{R}$ should be located in the region between $\mathcal{S}_2$ and $\mathcal{D}_2$.

Investigating the optimizing of RP for minimum EB, Fig. 13(a) shows that, if $P_1 = P_2 \gg P_R$, then the ANC-based $\mathcal{R}$ should be located in the neighbor of $\mathcal{D}_1$ and $\mathcal{D}_2$, whereas the PNC-based $\mathcal{R}$ should stay near $\mathcal{S}_1$ and $\mathcal{S}_2$. When $P_1 = P_2 \ll P_R$, the ANC-based relay should stay near $\mathcal{S}_1$ and $\mathcal{S}_2$, whereas the PNC-based relay should be located near $\mathcal{D}_1$ and

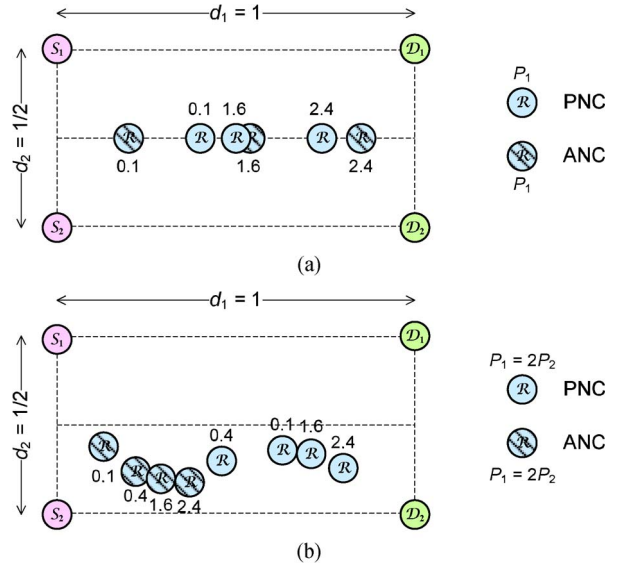


Fig. 12. Optimized relay location subject to minimizing ED with $R = 5$ b/s, $P_{\text{total}} = 5$ W, $d_{S_1D_1} = d_{S_2D_2} = 1$, and $d_{S_1S_2} = d_{D_1D_2} = 1/2$ (the number beside the node represents the value of $P_1$). (a) $P_1 = P_2$. (b) $P_1 = 2P_2$.

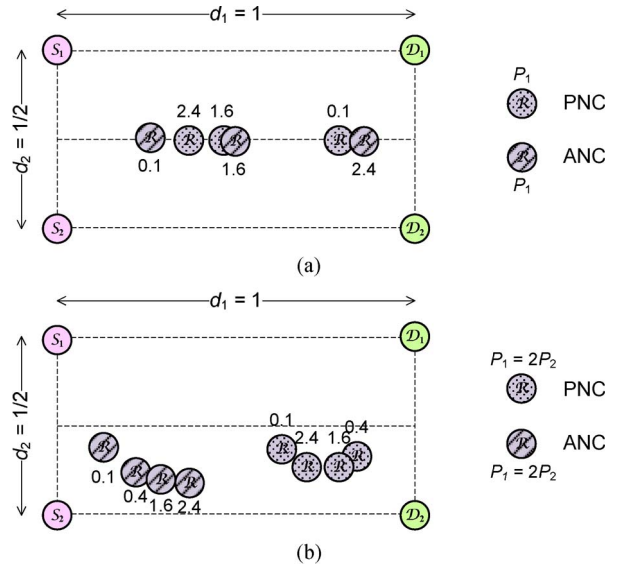


Fig. 13. Optimized relay location subject to minimizing EB with $R = 5$ b/s, $P_{\text{total}} = 5$ W, $d_{S_1D_1} = d_{S_2D_2} = 1$, and $d_{S_1S_2} = d_{D_1D_2} = 1/2$ (the number beside the node represents the value of $P_1$). (a) $P_1 = P_2$. (b) $P_1 = 2P_2$.

$\mathcal{D}_2$. For the scenarios when $P_1 > P_2$, it can be observed in Fig. 13(b) that the optimized locations of the ANC-based $\mathcal{R}$ and PNC-based $\mathcal{R}$ are similarly determined as in Fig. 12(b). Furthermore, the optimized locations for the ANC-based $\mathcal{R}$ are shown to be nearly similar for both objectives of minimum ED and minimum EB, whereas the optimized locations for the PNC-based $\mathcal{R}$ are different with respect to the objective functions. These nearly similar locations of the ANC-based $\mathcal{R}$ verify the statement in observation (O4).

## VII. Conclusion

In this paper, we have investigated the EDT of data transmissions in a WNCBN that consists of two source nodes, a relay node, and two destination nodes. HARQ-IR protocols with either PNC or ANC schemes have been considered for reliable data transmissions. The EDT has been derived for HARQ-IR protocols with PNC and ANC in WNCBNs by taking into account the effects of both relay location and power allocation. Additionally, we have derived the approximations of the EDTs for both nonrelay-aided and relay-aided transmissions in high- and low-power regimes. In the high-power regime, the use of the relay in both PNC and ANC schemes has been shown to have no advantage over the nonrelay-aided DT scheme. In the low-power regime, we have shown that the PNC scheme is more energy efficient than both the ANC and DT schemes when the relay node is located either at the center of the network or close to the destination nodes, whereas the DT scheme outperforms both the PNC and ANC schemes when the relay node is in the neighborhood of the source nodes. However, in the relaying schemes, the relay together with the source nodes can increase the diversity gain. Furthermore, based on the derived EDTs, algorithms for reducing the search region have been developed to find the optimal relay locations for the HARQ-IR protocols with PNC and ANC to minimize either the total delay or the total energy consumption in WNCBNs. Finally, numerical results have been provided to evaluate the energy efficiency of various HARQ-IR protocols, validate the EDT analysis, and determine the optimized relay locations for the minimum delay and the minimum energy consumption in WNCBNs. For future work, we will investigate the energy efficiency of different HARQ-IR protocols with respect to the whole power consumption at nodes. Moreover, the analytical solution for the RP problem with different HARQ-IR protocols will be investigated.

## Appendix A
## Proof of Lemma 2

It is noted that when $x$ is sufficiently small

$$\log(1+ax) \approx \frac{ax}{\ln 2} + O(x^2). \tag{50}$$

Thus, when $P \to 0$, applying the approximation in (50), we have

$$\log\left(1+[\gamma_{ii}]_j\right) \approx \frac{\left|[h_{ii}]_j\right|^2 P}{2\ln 2} \qquad \log\left(1+[\gamma_{ii'}]_j\right) \approx \frac{\left|[h_{ii'}]_j\right|^2 P}{2\ln 2}$$

where $i' = i-(-1)^i$, $i = 1, 2$. Since $E\{|h_{11}|^2\} = 1/d^{\nu}_{S_1D_1}$, $E\{|h_{22}|^2\} = 1/d^{\nu}_{S_2D_2}$, $E\{|h_{12}|^2\} = 1/d^{\nu}_{S_1D_2}$, $E\{|h_{21}|^2\} = 1/d^{\nu}_{S_2D_1}$, and $r_1 = r_2 = R$, we obtain

$$\bar{\kappa}_{\text{DT},1} \approx \frac{2R\ln 2}{P} \max\left\{d^{\nu}_{S_1D_1}, d^{\nu}_{S_1D_2}\right\} \tag{51}$$

$$\bar{\kappa}_{\text{DT},2} \approx \frac{2R\ln 2}{P} \max\left\{d^{\nu}_{S_2D_2}, d^{\nu}_{S_2D_1}\right\}. \tag{52}$$

Substituting (51) and (52) into (21) and (22) with $r_1 = r_2 = R$ and $P_1 = P_2 = P/2$, we obtain (24) and (25), respectively. The lemma is proven.

## APPENDIX B
## PROOF OF LEMMA 3

To evaluate the EDT of the HARQ-IR protocol with the PNC scheme in the low-power regime, let us consider (12) and (13).

When $P \to 0$, applying the approximation in (50) to $\kappa_{\mathrm{PNC,MA}}$, $\kappa_{\mathrm{PNC,DR}_i}$, and $\kappa_{\mathrm{PNC,BC}_i}$, $i = 1, 2$, given by (5), (7) and (10) with $r_i = R$ and $P_i = P_R = P/3$, we have

$$\bar{\kappa}_{\mathrm{PNC,MA}} \approx \frac{6R\ln 2}{P} \frac{d_{S_1R}^{\nu} d_{S_2R}^{\nu}}{d_{S_1R}^{\nu} + d_{S_2R}^{\nu}} \tag{53}$$

$$\bar{\kappa}_{\mathrm{PNC,DR}_1} \approx \frac{3R\ln 2}{P} d_{S_1D_1}^{\nu} \tag{54}$$

$$\bar{\kappa}_{\mathrm{PNC,DR}_2} \approx \frac{3R\ln 2}{P} d_{S_2D_2}^{\nu} \tag{55}$$

$$\bar{\kappa}_{\mathrm{PNC,BC}_i} \approx \frac{3R\ln 2}{P} d_{Ri}^{\nu}. \tag{56}$$

It is noted that $d_{S_1R}$ and $d_{3R}$ should be both less than $d_{S_1D_1}$ and $d_{S_2D_2}$. Thus

$$\frac{d_{S_1R}^{\nu} d_{S_2R}^{\nu}}{d_{S_1R}^{\nu} + d_{S_2R}^{\nu}} < \frac{d_{S_1D_1}^{\nu}}{2}, \quad \frac{d_{S_1R}^{\nu} d_{S_2R}^{\nu}}{d_{S_1R}^{\nu} + d_{S_2R}^{\nu}} < \frac{d_{S_2D_2}^{\nu}}{2}.$$

Accordingly, substituting (53)–(56) into (8), (9), and (11), we obtain

$$\bar{\kappa}_{\mathrm{PNC},S_1} \approx \frac{3R\ln 2}{P} d_{S_1D_1}^{\nu} \tag{57}$$

$$\bar{\kappa}_{\mathrm{PNC},S_2} \approx \frac{3R\ln 2}{P} d_{S_2D_2}^{\nu} \tag{58}$$

$$\bar{\kappa}_{\mathrm{PNC},1} \approx \frac{3R\ln 2}{P} \max\left\{d_{S_1D_1}^{\nu}, d_{S_2D_2}^{\nu}\right\} \tag{59}$$

$$\bar{\kappa}_{\mathrm{PNC},2} \approx \frac{3R\ln 2}{P} \max\left\{d_{RD_1}^{\nu}, d_{RD_2}^{\nu}\right\}. \tag{60}$$

Then, substituting (57)–(60) into (12) and (13) with $r_1 = r_2 = R$ results in (26) and (27). The lemma is proven.

## APPENDIX C
## PROOF OF LEMMA 4

Let us consider (19) and (20). When $P \to 0$, applying the approximation in (50) to $\kappa_{\mathrm{ANC}_i}$, $i = 1, 2$, given by (17) with $r_i = R$ and $P_i = P_R = P/3$, we have

$$\bar{\kappa}_{\mathrm{ANC}_i} \approx \frac{9R\ln 2}{P^2} d_{S_iR}^{\nu} d_{RD_i'}^{\nu} \tag{61}$$

where $i' = 2$ if $i = 1$ and $i' = 1$ if $i = 2$. Substituting (54), (55), and (61) into (18), we have

$$\bar{\kappa}_{\mathrm{ANC},S_1} \approx \max\left\{\frac{9R\ln 2}{P^2} d_{S_1R}^{\nu} d_{RD_2}^{\nu}, \frac{3R\ln 2}{P} d_{S_1D_1}^{\nu}\right\} \tag{62}$$

$$\bar{\kappa}_{\mathrm{ANC},S_2} \approx \max\left\{\frac{9R\ln 2}{P^2} d_{S_2R}^{\nu} d_{RD_1}^{\nu}, \frac{3R\ln 2}{P} d_{S_2D_2}^{\nu}\right\}. \tag{63}$$

Since $P \to 0$, it can be shown that

$$\frac{9R\ln 2}{P^2} d_{S_1R}^{\nu} d_{RD_2}^{\nu} > \frac{3R\ln 2}{P} d_{S_1D_1}^{\nu}$$
$$\frac{9R\ln 2}{P^2} d_{S_2R}^{\nu} d_{RD_1}^{\nu} > \frac{3R\ln 2}{P} d_{S_2D_2}^{\nu}.$$

Thus, (62) and (63) can be rewritten as

$$\bar{\kappa}_{\mathrm{ANC},S_1} \approx \frac{9R\ln 2}{P^2} d_{S_1R}^{\nu} d_{RD_2}^{\nu} \tag{64}$$

$$\bar{\kappa}_{\mathrm{ANC},S_2} \approx \frac{9R\ln 2}{P^2} d_{S_2R}^{\nu} d_{RD_1}^{\nu}. \tag{65}$$

Substituting (61), (64) and (65) into (19) and (20) with $r_1 = r_2 = R$ and $P_1 = P_2 = P_R = P/3$, we obtain (28) and (29). The lemma is proven.

## REFERENCES


[1] A. Sendonaris, E. Erkip, and B. Aazhang, "User cooperation diversity—Part I. System description," *IEEE Trans. Commun.*, vol. 51, no. 11, pp. 1927–1938, Nov. 2003.

[2] A. Sendonaris, E. Erkip, and B. Aazhang, "User cooperation diversity—Part II. Implementation aspects and performance analysis," *IEEE Trans. Commun.*, vol. 51, no. 11, pp. 1939–1948, Nov. 2003.

[3] J. Laneman, D. Tse, and G. Wornell, "Cooperative diversity in wireless networks: Efficient protocols and outage behavior," *IEEE Trans. Inf. Theory*, vol. 50, no. 12, pp. 3062–3080, Dec. 2004.

[4] K. Loa *et al.*, "IMT-advanced relay standards [WiMAX/LTE update]," *IEEE Commun. Mag.*, vol. 48, no. 8, pp. 40–48, Aug. 2010.

[5] Y. Yang, H. Hu, J. Xu, and G. Mao, "Relay technologies for WiMax and LTE-advanced mobile systems," *IEEE Commun. Mag.*, vol. 47, no. 10, pp. 100–105, Oct. 2009.

[6] Z. Sheng, K. Leung, and Z. Ding, "Cooperative wireless networks: From radio to network protocol designs," *IEEE Commun. Mag.*, vol. 49, no. 5, pp. 64–69, May 2011.

[7] S. Sharma, Y. Shi, Y. Hou, and S. Kompella, "An optimal algorithm for relay node assignment in cooperative *ad hoc* networks," *IEEE/ACM Trans. Netw.*, vol. 19, no. 3, pp. 879–892, Jun. 2011.

[8] M. Elhawary and Z. Haas, "Energy-efficient protocol for cooperative networks," *IEEE/ACM Trans. Netw.*, vol. 19, no. 2, pp. 561–574, Apr. 2011.

[9] R. Ahlswede, N. Cai, S.-Y. Li, and R. Yeung, "Network information flow," *IEEE Trans. Inf. Theory*, vol. 46, no. 4, pp. 1204–1216, Jul. 2000.

[10] R. Koetter and M. Medard, "An algebraic approach to network coding," *IEEE/ACM Trans. Netw.*, vol. 11, no. 5, pp. 782–795, Oct. 2003.

[11] S. Katti, D. Katabi, W. Hu, H. Rahul, and M. Medard, "The importance of being opportunistic: Practical network coding for wireless environments," in *Proc. Allerton*, Montecillo, Illinois, USA, Sep. 2005.

[12] S. Zhang, S. C. Liew, and P. P. Lam, "Hot topic: Physical-layer network coding," in *Proc. ACM MobiCom*, Los Angeles, CA, USA, Sep. 2006, pp. 358–365.

[13] S. Katti, S. Gollakota, and D. Katabi, "Embracing wireless interference: Analog network coding," in *Proc. ACM SIGCOMM*, Kyoto, Japan, Aug. 2007, pp. 397–408.

[14] S. Katti *et al.*, "XORs in the air: Practical wireless network coding," *IEEE/ACM Trans. Netw.*, vol. 16, no. 3, pp. 497–510, Jun. 2008.

[15] R. Louie, Y. Li, and B. Vucetic, "Practical physical layer network coding for two-way relay channels: Performance analysis and comparison," *IEEE Trans. Wireless Commun.*, vol. 9, no. 2, pp. 764–777, Feb. 2010.

[16] J. M. Park, S.-L. Kim, and J. Choi, "Hierarchically modulated network coding for asymmetric two-way relay systems," *IEEE Trans. Veh. Technol.*, vol. 59, no. 5, pp. 2179–2184, Jun. 2010.

[17] D. Nguyen, T. Tran, T. Nguyen, and B. Bose, "Wireless broadcast using network coding," *IEEE Trans. Veh. Technol.*, vol. 58, no. 2, pp. 914–925, Feb. 2009.

[18] P. Fan, C. Zhi, C. Wei, and K. Ben Letaief, "Reliable relay assisted wireless multicast using network coding," *IEEE J. Sel. Areas Commun.*, vol. 27, no. 5, pp. 749–762, Jun. 2009.

[19] Y. Liu, W. Chen, J. Ji, and J. Zhang, "Network-coded cooperation for multi-unicast with non-ideal source-relay channels," in *Proc. IEEE ICC*, Cape Town, South Africa, May 2010, pp. 1–5.

[20] F. Ye, S. Roy, and H. Wang, "Efficient data dissemination in vehicular *ad hoc* networks," *IEEE J. Sel. Areas Commun.*, vol. 30, no. 4, pp. 769–779, May 2012.

[21] Q. Yan, M. Li, Z. Yang, W. Lou, and H. Zhai, "Throughput analysis of cooperative mobile content distribution in vehicular network using symbol level network coding," *IEEE J. Sel. Areas Commun.*, vol. 30, no. 2, pp. 484–492, Feb. 2012.

[22] A. Zhan, C. He, and L. Jiang, "A channel statistic based power allocation in a butterfly wireless network with network coding," in *Proc. IEEE ICC*, Cape Town, South Africa, May 2010, pp. 1–5.

[23] Y. Qin and L.-L. Yang, "Delay comparison of automatic repeat request assisted butterfly networks," in *Proc. ISWCS*, York, U.K., Sep. 2010, pp. 686–690.
[24] J. Hu, P. Fan, K. Xiong, S. Yi, and M. Lei, "Cooperation-based opportunistic network coding in wireless butterfly networks," in *Proc. IEEE GLOBECOM*, Houston, TX, USA, Dec. 2011, pp. 1–5.
[25] A. Burr and J. Sykora, "Extended mappings for wireless network coded butterfly network," in *Proc. EW*, Vienna, Austria, Apr. 2011, pp. 1–7.
[26] S. B. Wicker, *Error Control Systems for Digital Communication and Storage*, Prentice-Hall, 1995.
[27] G. Caire and D. Tuninetti, "The throughput of hybrid-ARQ protocols for the Gaussian collision channel," *IEEE Trans. Inf. Theory*, vol. 47, no. 5, pp. 1971–1988, Jul. 2001.
[28] J. Choi, "On large deviations of HARQ with incremental redundancy over fading channels," *IEEE Commun. Lett.*, vol. 16, no. 6, pp. 913–916, Jun. 2012.
[29] J. Choi and D. To, "Energy efficiency of HARQ-IR for two-way relay systems with network coding," in *Proc. EW*, Poznan, Poland, Apr. 2012, pp. 1–5.
[30] Y. Liu and A. Petropulu, "Cooperative beamforming in multi-source multi-destination relay systems with SINR constraints," in *Proc. IEEE ICASSP*, Dallas, Texas, USA, Mar. 2010, pp. 2870–2873.
[31] Q.-T. Vien, B. G. Stewart, H. Tianfield, H. X. Nguyen, and J. Choi, "An efficient network coded ARQ for multisource multidestination relay networks over mixed flat fading channels," *Elsevier AEU Int. J. Electron. Commun.*, vol. 67, no. 4, pp. 282–288, Apr. 2013.
[32] Q.-T. Vien, B. G. Stewart, J. Choi, and H. X. Nguyen, "On the energy efficiency of HARQ-IR protocols for wireless network-coded butterfly networks," in *Proc. IEEE WCNC*, Shanghai, China, Apr. 2013, pp. 2559–2564.
[33] S. Zhang and S.-C. Liew, "Channel coding and decoding in a relay system operated with physical-layer network coding," *IEEE J. Sel. Areas Commun.*, vol. 27, no. 5, pp. 788–796, Jun. 2009.
[34] T. M. Cover and J. A. Thomas, *Elements of Information Theory*, 2nd ed. NJ, USA: Wiley, 2006.
[35] G. Wolberg, *Digital Image Warping*, 1st ed. Los Alamitos, CA, USA: Wiley-IEEE Comput. Soc., 1990.

**Quoc-Tuan Vien** (M'12) received the B.Sc. degree from Ho Chi Minh City University of Technology, Ho Chi Minh, Vietnam, in 2005; the M.Sc. degree from Kyung Hee University, Suwon, Korea, in 2009; and the Ph.D. degree from Glasgow Caledonian University, Glasgow, U.K., in 2012, all in radio engineering.

From 2005 to 2007, he was a Production System Engineer with Fujikura Fiber Optics Vietnam Company, Binh Duong, Vietnam. From 2010 to 2012, he was a Research and Teaching Assistant with the School of Engineering and Built Environment, Glasgow Caledonian University. In the Spring of 2013, he was Postdoctoral Research Assistant with the School of Science and Technology, Nottingham Trent University, Nottingham, U.K. He is currently a Lecturer of computing and communications engineering with the School of Science and Technology, Middlesex University, London, U.K. His research interests include multiple-input–multiple-output systems and techniques, network coding, relay networks, and cognitive radio networks.

Dr. Vien is a member of the Institution of Engineering and Technology.

**Huan X. Nguyen** (M'06) received the B.Sc. degree from Hanoi University of Technology, Hanoi, Vietnam, in 2000 and the Ph.D. degree from the University of New South Wales, Sydney, Australia, in 2007.

From 2000 to 2003, he was with Vietnam Television, where he focused on designing a terrestrial digital television network. In 2007, he joined the Institute of Advanced Telecommunications, Swansea University, Swansea, U.K., as a Research Officer. From 2008 to 2010, he was a Lecturer with the School of Engineering and Computing, Glasgow Caledonian University, Glasgow, U.K. He is currently a Senior Lecturer with the School of Engineering and Information Sciences, Middlesex University, London, U.K. His research interests include multiple-input–multiple-output techniques, multicarrier systems, and relay communications.

**Brian G. Stewart** (M'08) received the B.Sc. (Hons) degree and the Ph.D. degree from the University of Glasgow, Glasgow, U.K., in 1981 and 1985, respectively, and the BD (Hons) degree from The University of Aberdeen, Aberdeen, U.K., in 1994.

In 1985, he was appointed a Lecturer with the School of Electronic and Electrical Engineering, Robert Gordon University, Aberdeen. Since 1998, he has been with Glasgow Caledonian University, Glasgow, where he is currently a Professor with the School of Engineering and Built Environment. He has held numerous government and industrial research grants and has published numerous research papers in journals and international conferences. He also holds a number of patents in the fields of communication systems and high-voltage instrumentation. He has more than 25 years of teaching and research experience. His research interests include communication systems and high-voltage partial discharge.

Dr. Stewart is a Chartered Engineer and a member of the Institution of Engineering and Technology.

**Jinho Choi** (SM'13) was born in Seoul, Korea. He received the B.E. degree (*magna cum laude*) in electronics engineering from Sogang University, Seoul, in 1989 and the M.S.E. and Ph.D. degrees in electrical engineering from Korea Advanced Institute of Science and Technology, Daejeon, Korea, in 1991 and 1994, respectively.

He is currently a Professor with the School of Information and Communications, Gwangju Institute of Science and Technology (GIST), Gwangju, Korea. Prior to joining GIST, he was with the College of Engineering, Swansea University, Swansea, U.K., as a Professor/Chair of wireless communications. He is the author of two books published by Cambridge University Press in 2006 and 2010. His research interests include wireless communications and array/statistical signal processing.

Dr. Choi currently serves as an Associate Editor for IEEE COMMUNICATIONS LETTERS and has been serving as an Editor for the *Journal of Communications and Networks* since 2005. He also served as an Associate Editor for the IEEE TRANSACTIONS ON VEHICULAR TECHNOLOGY from 2005 to 2007 and for the *ETRI journal*. He received the 1999 Best Paper Award for Signal Processing from the European Association for Signal Processing and the 2009 Best Paper Award at the Wireless Personal Multimedia Communications Symposium.

**Wanqing Tu** (M'04) received the Ph.D. degree in computer science from the City University of Hong Kong, Kowloon, Hong Kong, in 2006.

She is currently a Reader with the School of Computing Science and Digital Media, The Robert Gordon University, Aberdeen, U.K. From 2008 to 2012, she was a Senior Lecturer with Glyndwr University, Wrexham, U.K., and from 2012 to 2013, with Nottingham Trent University, Nottingham, U.K. Her research interests include next-generation multimedia networking, wireless multihop networks, mobile computing, cognitive radio networks, overlay networks, and parallel and distributed systems.

Dr. Tu was an Executive Committee Member of The IET Multimedia Communications Network from 2011 to 2013. She received a Research Exchange Award from the Royal Academy of Engineering, London, U.K., in 2013, an IRCSET Embark Initiative Postdoctoral Research Fellowship, Ireland, in 2006, and a Best Paper Award from the International Conference on Communications, Networking and Mobile Computing in 2005.